CRCLEME
Cooperative Research Centre for
Landscape Evolution & Mineral Exploration

CSIRO
EXPLORATION
AND MINING

AMIRA
Australian Mineral Industries Research Association Limited ACN 004 448 266

OPEN FILE
REPORT
SERIES

# SPECTRAL PROPERTIES OF MUSCOVITE- AND PARAGONITE-BEARING ROCKS AND SOILS FROM THE PANGLO GOLD DEPOSIT, ORA BANDA REGION, WESTERN AUSTRALIA

*T.J. Cudahy, K.M. Scott and A.R. Gabell*

**CRC LEME OPEN FILE REPORT 66**

February 1999

(CSIRO Division of Exploration Geoscience Report 234R, 1992.
Second impression 1999)

AMIRA
Australian Mineral Industries Research Association Limited ACN 004 448 266

CRCLEME
Cooperative Research Centre for Landscape Evolution & Mineral Exploration

CSIRO
EXPLORATION AND MINING

# SPECTRAL PROPERTIES OF MUSCOVITE- AND PARAGONITE-BEARING ROCKS AND SOILS FROM THE PANGLO GOLD DEPOSIT, ORA BANDA REGION, WESTERN AUSTRALIA

*T.J. Cudahy, K.M. Scott and A.R. Gabell*

**CRC LEME OPEN FILE REPORT 66**

February 1999

(CSIRO Division of Exploration Geoscience Report 234R, 1992.
Second impression 1999)



CRC LEME is an unincorporated joint venture between The Australian National University, University of Canberra, Australian Geological Survey Organisation and CSIRO Exploration and Mining
*Headquarters:* CRC LEME c/o CSIRO Exploration and Mining, Private Bag, PO Wembley, Western Australia, 6014

## RESEARCH ARISING FROM CSIRO/AMIRA REGOLITH GEOCHEMISTRY PROJECTS 1987-1993

In 1987, CSIRO commenced a series of multi-client research projects in regolith geology and geochemistry which were sponsored by companies in the Australian mining industry, through the Australian Mineral Industries Research Association Limited (AMIRA). The initial research program, "Exploration for concealed gold deposits, Yilgarn Block, Western Australia" (1987-1993) had the aim of developing improved geological, geochemical and geophysical methods for mineral exploration that would facilitate the location of blind, buried or deeply weathered gold deposits. The program included the following projects:

**P240: Laterite geochemistry for detecting concealed mineral deposits (1987-1991).** Leader: Dr R.E. Smith.
Its scope was development of methods for sampling and interpretation of multi-element laterite geochemistry data and application of multi-element techniques to gold and polymetallic mineral exploration in weathered terrain. The project emphasised viewing laterite geochemical dispersion patterns in their regolith-landform context at local and district scales. It was supported by 30 companies.

**P241: Gold and associated elements in the regolith - dispersion processes and implications for exploration (1987-1991).** Leader: Dr C.R.M. Butt.
The project investigated the distribution of ore and indicator elements in the regolith. It included studies of the mineralogical and geochemical characteristics of weathered ore deposits and wall rocks, and the chemical controls on element dispersion and concentration during regolith evolution. This was to increase the effectiveness of geochemical exploration in weathered terrain through improved understanding of weathering processes. It was supported by 26 companies.

These projects represented "an opportunity for the mineral industry to participate in a multi-disciplinary program of geoscience research aimed at developing new geological, geochemical and geophysical methods for exploration in deeply weathered Archaean terrains". This initiative recognised the unique opportunities, created by exploration and open-cut mining, to conduct detailed studies of the weathered zone, with particular emphasis on the near-surface expression of gold mineralisation. The skills of existing and specially recruited research staff from the Floreat Park and North Ryde laboratories (of the then Divisions of Minerals and Geochemistry, and Mineral Physics and Mineralogy, subsequently Exploration Geoscience and later Exploration and Mining) were integrated to form a task force with expertise in geology, mineralogy, geochemistry and geophysics. Several staff participated in more than one project. Following completion of the original projects, two continuation projects were developed.

**P240A: Geochemical exploration in complex lateritic environments of the Yilgarn Craton, Western Australia (1991-1993).** Leaders: Drs R.E. Smith and R.R. Anand.
The approach of viewing geochemical dispersion within a well-controlled and well-understood regolith-landform and bedrock framework at detailed and district scales continued. In this extension, focus was particularly on areas of transported cover and on more complex lateritic environments typified by the Kalgoorlie regional study. This was supported by 17 companies.

**P241A: Gold and associated elements in the regolith - dispersion processes and implications for exploration.** Leader: Dr. C.R.M. Butt.
The significance of gold mobilisation under present-day conditions, particularly the important relationship with pedogenic carbonate, was investigated further. In addition, attention was focussed on the recognition of primary lithologies from their weathered equivalents. This project was supported by 14 companies.

Although the confidentiality periods of the research reports have expired, the last in December 1994, they have not been made public until now. Publishing the reports through the CRC LEME Report Series is seen as an appropriate means of doing this. By making available the results of the research and the authors' interpretations, it is hoped that the reports will provide source data for future research and be useful for teaching. CRC LEME acknowledges the Australian Mineral Industries Research Association and CSIRO Division of Exploration and Mining for authorisation to publish these reports. It is intended that publication of the reports will be a substantial additional factor in transferring technology to aid the Australian Mineral Industry.

This report (CRC LEME Open File Report 66) is a Second impression (second printing) of CSIRO Division of Exploration Geoscience Restricted Report 234R, first issued in 1992, which formed part of the CSIRO/AMIRA Projects P243 and 241A.

**Copies of this publication can be obtained from:**
The Publication Officer, c/- CRC LEME, CSIRO Exploration and Mining, PMB, Wembley, WA 6014, Australia. Information on other publications in this series may be obtained from the above or from http://leme.anu.edu.au/

**Cataloguing-in-Publication:**
Cudahay, T.J.
Spectral properties of muscovite- and paragonite-bearing rocks and soils from the Panglo Gold Deposit, Ora Banda Region, Western Australia
ISBN 0 642 28262 5
1. Gold - Western Australia 2. Geochemistry 3. Remote sensing
I. Scott, K.M. II. Gabell, A.R. III. Title
CRC LEME Open File Report 66.
ISSN 1329-4768

## FRONTISPIECE

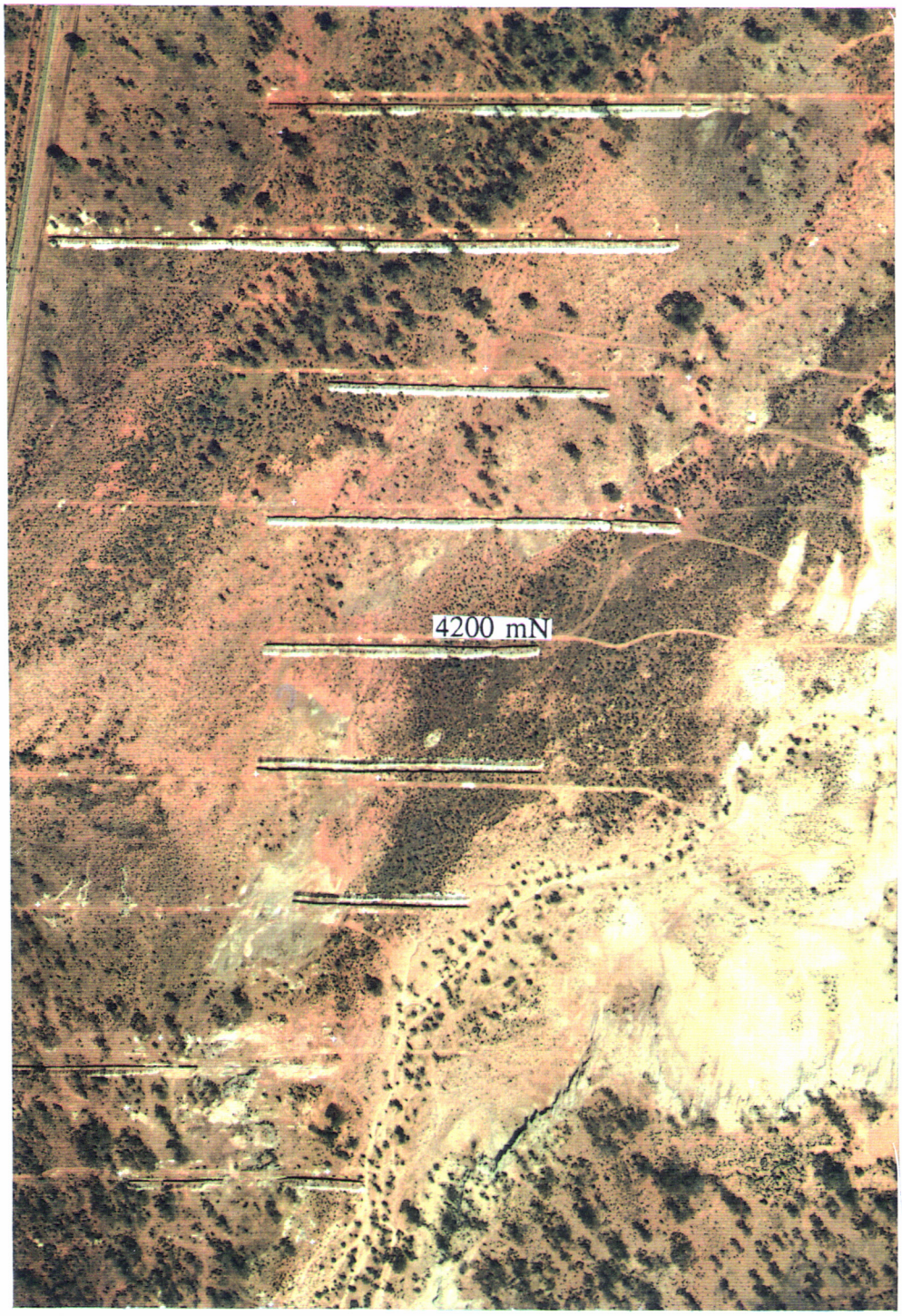


Colour aerial photograph of the Panglo area showing bright areas of salt-scalding and numerous costeans approximating the zone of supergene gold mineralisation. Line 4200 mN, along which many of the samples were collected, is indicated. Approximate scale is 1:8000 and grid north is up the page. Air photograph probably taken by Kevron Air Surveys 15th Dec 1986, Photo 9115, published with permission of Goldfields Exploration Pty Ltd.

## PROJECT LEADERS PREFACE

The CSIRO-AMIRA Research Program "Exploration for Concealed Gold Deposits, Yilgarn Craton, Western Australia" has as its overall aim the development of improved geological, geochemical and geophysical methods for mineral exploration that will facilitate the location of blind, concealed, or deeply weathered gold deposits. The research has been undertaken by three modules - Laterite Geochemistry (AMIRA Project P240), Weathering Processes (AMIRA Project P241), and Remote Sensing (AMIRA Project P243).

The Remote Sensing Project's primary aim is to develop, evaluate and demonstrate new remote sensing techniques tailored to exploration in the deeply weathered terrains of Western Australia. An important part of this strategy is determining the spectral characteristics of areas of gold mineralisation as this information can assist in the selection, processing and interpretation of spectral data.

There have been six detailed studies on the visible to shortwave infrared reflectance characteristics of a wide range of Yilgarn regolith materials, including weathered gold alteration systems and unmineralised geology (160R, 169R, 234R, 235R, 240R and 244R). These spectral studies have generally proceeded in conjunction with mineralogical and geochemical investigations by P240 and P241 scientists so that relationships have been established between spectral reflectance and mineralogical/geochemical/physical information. This has facilitated a more quantitative thematic analysis of the spectral data.

This study details the results from one of these collaborative investigations for the Panglo gold deposit and focuses on the spectral detection of potassic micas, a common product of gold-related hydrothermal alteration.

A.R. Gabell
Project Leader

September, 1992

## SUMMARY

Gold exploration in the Yilgarn Craton would be greatly assisted if minerals, diagnostic of gold-related alteration, were developed at the surface and detectable using spectral remote sensing methods. One group of minerals that may satisfy this need are the potassic micas which are often found in weathered surface materials overlying zones of potassic, gold-related, hydrothermal alteration. These minerals exhibit characteristic absorptions in the 0.4 to 2.5 $\mu$m wavelength region, though it was not clear whether the natural abundances of these minerals are sufficient to produce these absorptions. An answer to this problem was the first objective of this study. The second objective of the study was to determine whether different species of mica could be discriminated.

These problems were investigated using a suite of surface and subsurface samples of weathered mafic rock, shale and soil collected from the Panglo gold deposit, Western Australia. The Panglo deposit was interesting as the alteration comprised muscovite (K-bearing mica), associated with mineralisation, and paragonite (Na-bearing mica), in areas peripheral to mineralisation. Therefore, spectral discrimination of these two mica minerals could theoretically better define the limits of gold mineralisation.

The spectral investigation concentrated on the wavelengths of the 1.4 and 2.2 $\mu$m absorptions (hypothetically provide information on the composition of micas related to the size and composition of the mica unit-cell), and the depth of the 2.35 $\mu$m absorption (provides information about the abundance of mica). The geometry of the 1.4 and 2.2 $\mu$m absorptions were not considered as these are strongly affected by other clays, such as kaolinite and smectite. Some consideration was given to the associated spectral mineralogy (nature of other clays, sulphates, water) and possible relationships to the character of the regolith.

The results showed the wavelengths of the OH-related absorption at 1.4 $\mu$m and the Al-OH 2.2 $\mu$m absorption are approximately 10 nm longer than expected for either muscovite or paragonite. There is also no pattern between these parameters from paragonite-rich to muscovite-rich. These negative results can be caused by mixing with other 2.2 $\mu$m absorbing, Al-OH minerals, such as kaolinite. The spectrum of a kaolinite-poor, muscovite-rich shale sample showed wavelengths expected for muscovite.

The concentration of $K_2O$ was used as a quantitative measure for the abundance of muscovite and was compared with the depth of the 2.35 $\mu$m absorption. The results showed significant correlation, though a threshold muscovite concentration of approximately 3% $K_2O$ is required, below which the 2.35 $\mu$m absorption is no longer distinguishable in the reflectance spectra. This threshold abundance equates to approximately 20% muscovite (by weight). The only exceptions to this relationship were exhibited by the spectra of quartz-rich shales (>60% $SiO_2$) which showed the threshold abundance can be as little as 1% $K_2O$. This lower threshold is probably related to the relatively transparent nature of quartz.

The natural $K_2O$ abundances of the weathered mafic subcrop were sufficient to produce recognisable absorption at 2.35 $\mu$m. Therefore, mica-bearing, mafic outcrop or float (if present), can be detected using spectral techniques. However, the soils did not show this absorption apparently because these contained $<1\%$ $K_2O$ (by weight). Therefore, spectral sensing of soils derived from mica-rich, mafic rocks is unlikely to show mica-related absorption at 2.35 $\mu$m.

A relationship, analogous to that between the $K_2O$ content and the depth of the 2.35 $\mu$m absorption, could not be established for the $Na_2O$ and paragonite abundances. This is because the samples contained halite.

The reflectance data show different spectral properties for the mafic subcrop, soils and sedimentary subcrop. The mafic subcrop are characterised by strong absorption at 1.395, 1.411, 2.165, 2.318 and 2.386 $\mu$m, producing absorption doublets at 1.4 and 2.2 $\mu$m. These properties are typical of well-crystalline kaolinite. The soils are characterised by weaker absorptions at these wavelengths, producing poor absorption doublets, indicating more poorly crystalline kaolinite. The soil spectra also show small absorptions at 1.46 and 2.25 $\mu$m, possibly caused by water, Fe- or Si-cations in the kaolinite structure (typical of more poorly crystalline clay). The shale subcrop show weak to nonexistent development of the kaolinite absorption doublets.

The results from this study have limited application to gold exploration strategies. The most important result is the requirement for $3\%$ $K_2O$ in a material (contained in potassic mica) before the mica-related absorption at 2.35 $\mu$m becomes apparent in the reflectance spectra. If soils dominate the surface materials over mica-bearing gold mineralisation, as is the case at Panglo, then remote sensing techniques (at these wavelengths) are not practical, unless the soils are quartz-rich (quartz-rich soils are not likely to be associated with mafic/ultramafic rocks). The most appropriate application of these results is in the field where a spectrometer could be used to log the presence and abundance of mica in subcrop and drill core. Further work is required to establish whether mica-bearing, mafic saprock is spectrally characterised by well-crystalline kaolinite and K-bearing mica.

## CONTENTS

## 1.0 INTRODUCTION

Gold exploration in the Yilgarn Craton using spectral sensing techniques is made difficult by the deep weathering of the regolith and the limited number of detailed spectral studies on weathered materials from this environment. To address this problem, a significant part of the P243 research activity has concentrated on characterising the 0.4 to 2.5 $\mu$m reflectance properties of weathered gold deposits and background areas (Cudahy and others, 1992a and 1992b; Cudahy, 1992b; Gozzard and Tapley, 1992). This wavelength region is useful for addressing these problems as many primary, alteration and "weathering" minerals have characteristic absorptions in this region (Hunt and Salisbury, 1970; Clark and others, 1990). It is also well covered by a variety of field, airborne and space-borne, spectral sensing systems, which are available, or are soon to be available, to the exploration industry.

Many of the hydrothermal gold deposits in the Archaean greenstone belts of the Yilgarn Craton are associated with potassic metasomatism (Groves and others, 1985; Clark and others, 1988; Butt and others, 1991), commonly showing the presence of potassic micas (muscovite, Na-muscovite, hydromuscovite, fuchsite, sericite). Potassic micas (K-micas) are relatively resistant to erosion and weathering and so often persist through the weathered mantle to the surface (Robertson and others, 1990; Butt, 1991; Butt and others, 1991; Lintern and Scott, 1991). Thus, K-micas represent a potential "indicator" mineral for gold mineralisation that could be targeted by explorationists using spectral sensing techniques (remote or proximal).

However, there are two problems that affect the use of K-micas as an "indicator" mineral. Firstly, K-micas are common in non-mineralised rocks, such as felsic intrusives and sediments, though it is unusual to find K-micas developed in mafic or ultramafic rocks unless they have been affected by potassic metasomatism. Secondly, it is not known whether the natural abundances of K-mica at the surface are sufficient to produce recognisable absorptions (at these wavelengths).

These problems are partly addressed in this study of weathered surface and subsurface materials from the Panglo gold deposit. The Panglo deposit was selected because there is K-mica alteration of mafic rocks and there is an interesting spatial association between different micas species. Paragonite (Na-bearing mica) is developed peripheral to the mineralisation zone whereas muscovite (K-bearing mica) is developed over gold mineralisation and into the marginal areas. Therefore, this style of mica alteration could potentially be used to better define the limits of gold mineralisation in mafic host rocks.

## 2.0 OBJECTIVES

The main objectives of this study were:

1. To measure the reflectance spectra of muscovite- and paragonite-bearing rocks and soils collected from various levels of the regolith profile associated with gold mineralisation at Panglo;

2. To quantitatively relate the spectral information with mineralogical and geochemical data; and

3. To establish spectral detection limits for muscovite and paragonite discrimination in natural, weathered materials.

## 3.0 LOCATION, GEOLOGY, AND GEOMORPHOLOGY

The Panglo gold mine is located 30 km NNW of Kalgoorlie in the Eastern Goldfields of Western Australia (Figure 1). The climate of the region is semi arid with a Mediterranean tendency (winter rainfall maximum). The vegetation is a mosaic of predominantly eucalypt woodlands (Plate 1) becoming open with a saltbush and bluebush understorey on the more calcareous soils (Plate 2). The topographic relief of the area is generally flat.

The local geology is part of a northwest-southeast-trending Archaean greenstone belt comprising mafic, ultramafic and sedimentary rocks (Figure 1). Primary gold mineralisation developed within an 800 metre wide NNW-trending shear zone intersecting mafic volcanics and shales (Scott, 1990; Scott and Dotter, 1990; Lintern and Scott, 1991). Paragonite appears to be restricted to areas peripheral to the mineralisation zone whereas muscovite is developed over mineralisation (Scott, 1990; Lintern and Scott, 1991). Supergene gold mineralisation has developed in the weathered mantle.

Outcropping rocks are rare with weathering extending to a depth of approximately 60m. Clay and/or iron-rich lithorelics appear to be common, especially below the surface. The soils are thin (less than 0.5 m deep) and clay-rich, often with a thin, surficial layer of iron-stained sand. Many of the soils also show evidence of colluvial/fluvial transportation. Broad ephemeral drainage systems are located adjacent to, and encroaches over the southern part of, the zone of mineralisation (Figure 1).

## 4.0 SAMPLE COLLECTION AND PREPARATION

Twentysix surficial soil and 17 samples of subcrop from line 4200 mN (Figure 1) were collected prior to major modification of the surface environment by mining. This line overlies supergene and possibly primary mineralisation within weathered mafic and sedimentary rocks. Soils were collected from the top 0.1 m and the subcropping rock was collected from a depth of 0.3 m within an adjoining costean. Where possible, organic matter was removed from the soil samples.

Seven samples were also collected from drill holes (PSRC172, PSRC238, PSRC239 and PSRC341) by Bob Howard (Pancontinental Mining Ltd). These samples were from various depths (ranging from 5-57 m) and comprised mineralised and barren mafic and sedimentary rocks. These drill core samples were selected as they represent good examples of paragonite-rich and muscovite-rich materials.

There was no preparation of the samples before spectral measurement though preparation was required for the analytical measurements (Section 5.0).

Plate 1: Eucalyptus and Casuarina open woodland.

Plate 2: Bluebush and grasses over calcareous soils with salt-scalded areas in the midground. Looking west towards the costeans along 4200 mN.

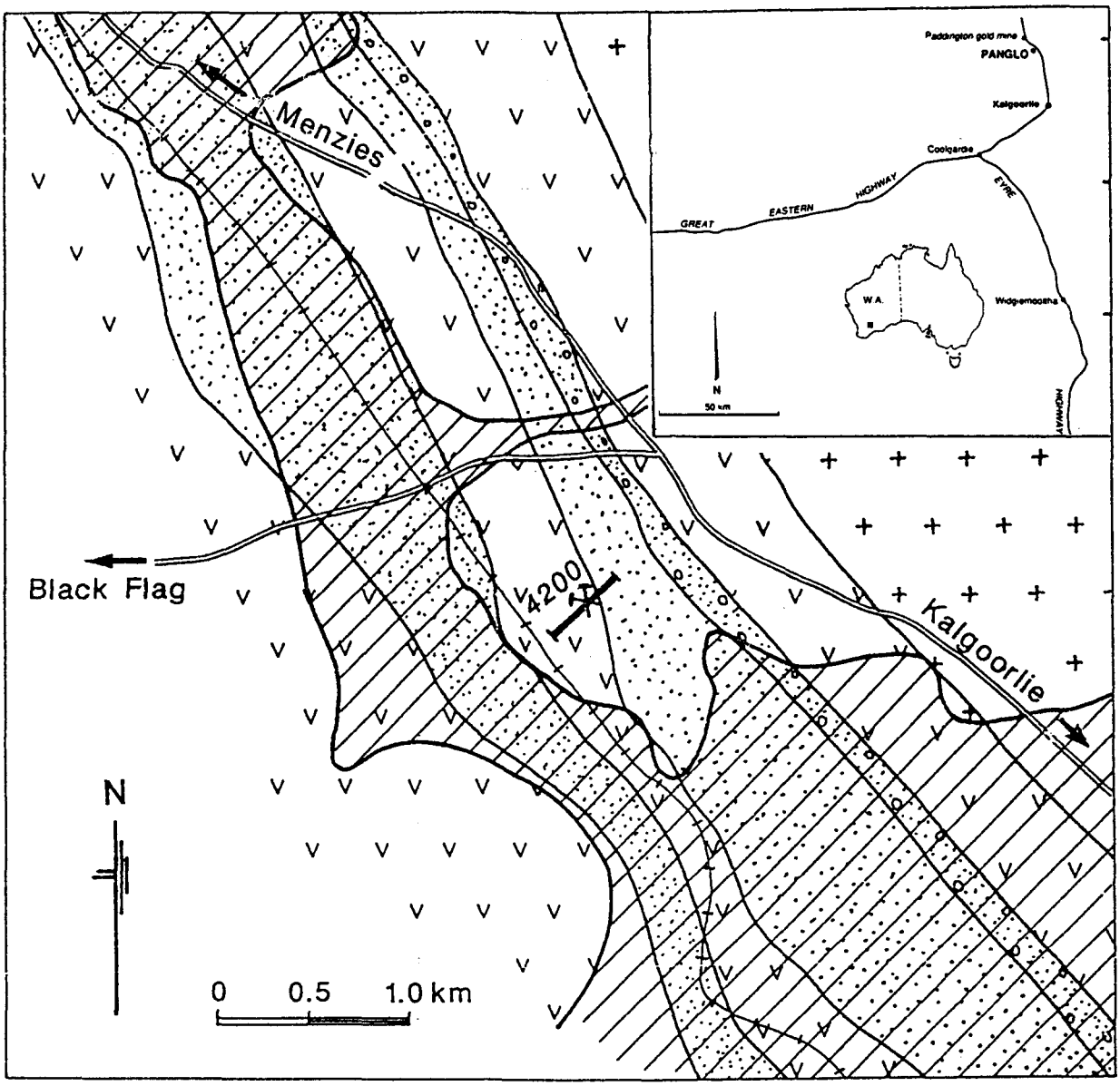


Tertiary Palaeochannel

Granite

Volcanic Agglomerate

Shale

Mafic and Ultramafic Volcanics

Railway

Roads

Line and northing

Panglo Deposit

**Figure 1:** Location of the Panglo study area and the local geology. The location of the sample line 4200 mN is shown (after Scott and Dotter, 1990 and Lintern and Scott, 1991).

## 5.0 ASSOCIATED MINERALOGICAL INFORMATION

The samples for spectral measurement were crushed to less than 75 $\mu$m and analysed for their mineralogy and geochemistry (Scott, 1989; Lintern and Scott, 1991) using X-ray diffraction (XRD), X-ray florescence (XRF) and inductively coupled plasma (ICP). The mineralogy was determined using a Phillips PW1050 X-Ray Diffractometer with CuK radiation at 40 kV. The heights of major XRD peaks, relative to a standard, provided an estimate of the mineral abundances. The $Na_2O$ contents were measured using a Phillips PW 1200C XRF instrument and the $K_2O$ contents were measured using either a Labtem or Hilger E-100 ICP. Electron microprobe analyses were made using a Camebax wavelength dispersive instrument. These analyses defined the composition of the octahedral and tetrahedral cations in individual mica crystals (Section 6.0) so as to establish the precise mineralogy within this mineral group.

## 6.0 FUNDAMENTALS OF SPECTRAL MINERALOGY

The micas produce absorptions in the 1.3 to 2.5 $\mu$m wavelength region related to vibrations of mineralogical, molecular bonds. For example, absorption at 2.2 $\mu$m is related to a combination tone of the OH-bond fundamental stretch with the Al-O-H fundamental bending mode (Hunt and Ashley, 1979). These particular bonds are present in dioctahedral silicates which consist of layers of octahedrally coordinated cations (primarily $Al^{3+}$) sandwiched between two layers of $(Si,Al)O_4$ tetrahedra (Figure 2). Trioctahedral silicates have absorption at slightly longer wavelengths (near 2.3 $\mu$m) because the vibrations are associated with octahedrally coordinated $Mg^{2+}$, $Fe^{2+}$ and/or $Li^{2+}$. Additional hydroxyl ions, together with apical tetrahedra oxygen atoms, comprise the octahedral coordination to the octahedral cations with the net negative charge of these layers balanced by planes (interlayers) of cations ($K^+$, $Na^+$, $H_3O^+$) in twelve-fold coordination (Deer and others, 1977). Muscovite has interlayers occupied by $K^+$ whereas paragonite has interlayers occupied by $Na^+$ with both minerals containing octahedrally coordinated $Al^{3+}$.

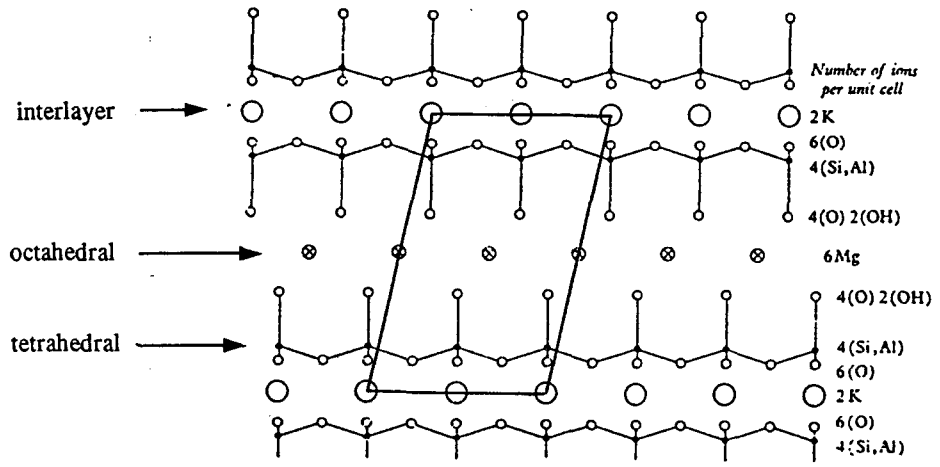


**Figure 2:** The generalised structure of mica viewed along the y-axis showing the arrangement of oxygens, hydroxyls, tetrahedral cations, octahedral cations and interlayer cations (after Deer and others, 1977).

The 1.3 to 2.5 $\mu$m wavelength reflectance spectra of pure muscovite and paragonite (Figure 3a and 3g, respectively) show absorptions at 1.4, 2.2, 2.35 and 2.45 $\mu$m. The interlayer $K^+$ and $Na^+$ cations in muscovite and paragonite (respectively) have a very small affect on the energy of vibration of the "active" bonds at these wavelengths. The Na ion is smaller than the K ion which causes a slight difference in the size of the unit cell (Figure 2) and consequently causes a subtle shift in the energy of vibration of the bonds associated with the octahedrally coordinated $Al^{3+}$. These subtle changes provide an explanation for the apparent differences in the wavelengths of the muscovite absorptions (at 1.407, 2.202 and 2.348 $\mu$m; Figure 3a) and the slightly shorter paragonite absorptions (at 1.404, 2.197 and 2.337 $\mu$m; Figure 3g). There are absorptions related to the interlayer cations outside of this wavelength region in the far infrared (Prost and Laperche, 1990).

Illite is a common weathering product of muscovite. Illite comprises a crystal structure essentially that of muscovite with fewer interlayer cations (K), a capacity for interlayer water and other cations and less regularity to the lattice stacking (Deer and others, 1977). These differences affect the spectral properties. The reflectance spectrum of pure illite (Figure 3c) shows major absorptions similar to muscovite/paragonite (Figure 3a and 3g), though illite can have water absorption at 1.9 $\mu$m and slightly longer wavelengths to the 1.4 and 2.2 $\mu$m absorptions, possibly related to an increase in the size of the unit cell.

## 7.0 REFLECTANCE MEASUREMENT AND PROCESSING

The detection of muscovite and paragonite, using 1.3 to 2.5 $\mu$m reflectance data, required a high spectral resolution spectrometer able to discriminate changes in wavelength of less than 10 nm. For this reason, the PIMA-II was selected because it offers high spectra resolution.

### 7.1 Spectrometer

The PIMA-II (Portable Infrared Mineral Analyser), developed by CSIRO/Integrated Spectronics, is a portable hand-held unit (2.5 kg) that measures bidirectional reflectance (relative to a polished gold plate standard) between 1.3 to 2.5 $\mu$m. The spectral resolution is 7-10 nm with a sampling interval of 2 or 4 nm. Data acquisition time for each spectra is 20-30 secs in 2 nm sample mode. No external light is required as there is an inbuilt source of illumination.

### 7.2 Spectral Processing and Analysis

The reflectance data were ported to an IBM-compatible PC and processed using PCSpectra. PCSpectra is a software package, developed by the CSIRO, for the processing and analysis of spectral data. The spectra were processed to generate hull quotient spectra (Green and Craig, 1985) so that subtle absorption features could be enhanced. The depth of the 2.35 $\mu$m absorption was gauged using a PCSpectra routine, called "Feature Extraction", which uses hull quotient spectra. The 2.35 $\mu$m absorption depth was also measured using a ratio of reflectances taken from the absorption shoulders (2.338 + 2.368 $\mu$m) divided by the reflectance at the base of the absorption.

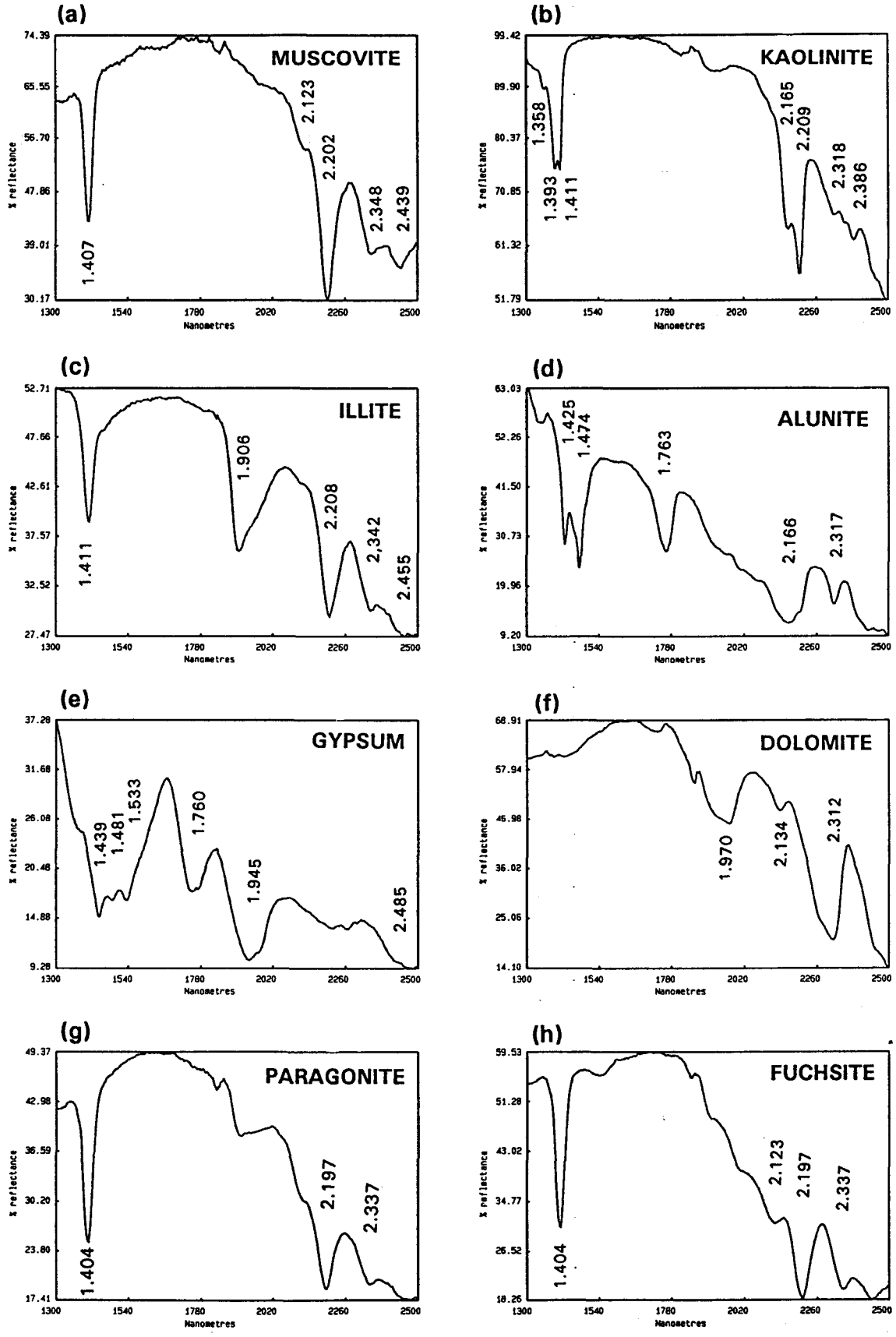


**Figure 3:** The reflectance spectra of various pure minerals (from the CSIRO Remote Sensing Group Spectral Library).

## 7.3 Comparisons Between Spectral and Physicochemical Data

There may be significant problems in relating reflectance information with other analytical data as the reflectance information is derived from the surface of a material (outer few microns; Buckingham and Sommer, 1983) whereas XRD, XRF and ICP techniques measure the "bulk" properties. Another problem is that reflectance information is often taken from natural surfaces whereas the other analytical techniques usually require homogenised powders. Therefore, care should be given to interpreting the importance of relationships (or lack of) between spectral information and these other data sets.

The major physicochemical parameters required for comparison with the reflectance data were the abundances of muscovite and paragonite. However, the XRD technique used to measure this information (Section 5.0) only provided relative abundances. It was decided that a better quantitative measurement of the muscovite content would be derived from the ICP $K_2O$ contents. This is possible if all the $K_2O$ is contained in muscovite. Unfortunately, a similar assumption is not valid for paragonite and the $Na_2O$ contents, mainly because halite (and to a lesser degree feldspar) is common in these samples. Therefore, without determining the Cl contents to allow for Na present in halite, there was no suitable measurement of the paragonite concentration for comparison with the spectral information.

The analysis of the drill core, soils and subcrop were considered separately for several reasons. The drill core samples were selected because they represent the "best" examples of muscovite-rich and paragonite materials. The spectra of these samples were compared with the associated SEM results for the elemental composition of the interlayer and octahedral layers of mica minerals (White and others, 1961; Vedder and McDonald, 1962; Rosenquist and Jorgensen, 1963; Vedder, 1964). The subcrop samples included a variety of weathered mafic volcanic and shale rocks with and without potassic alteration. This variety provided a way to test the spectral separation of these lithologies. The soils were of interest because they are often the only material present at the surface and so are the most relevant to surface exploration techniques, such as remote sensing.

Two parameters were considered to show significant correlation if their $r^2$ value exceeded the 99% confidence level for the number of samples considered in the analysis (assuming gaussian distribution).

# 8.0 RESULTS AND DISCUSSION

The PIMA-II reflectance spectra are presented in Appendix 1 together with the associated analyses for the mineralogy and geochemistry and the hull quotient depths for the 2.35 $\mu$m absorption (if present). The spectra show various absorptions. These are listed and given an explanation for their development in Appendix 2.

The majority of the spectra show evidence for kaolinite absorptions located at 1.395, 1.41, 2.165, 2.2, 2.318 and 2.386 $\mu$m (Figure 3b) and water absorption at 1.9 $\mu$m. The XRD analyses also showed kaolinite to be present in these samples though many of the

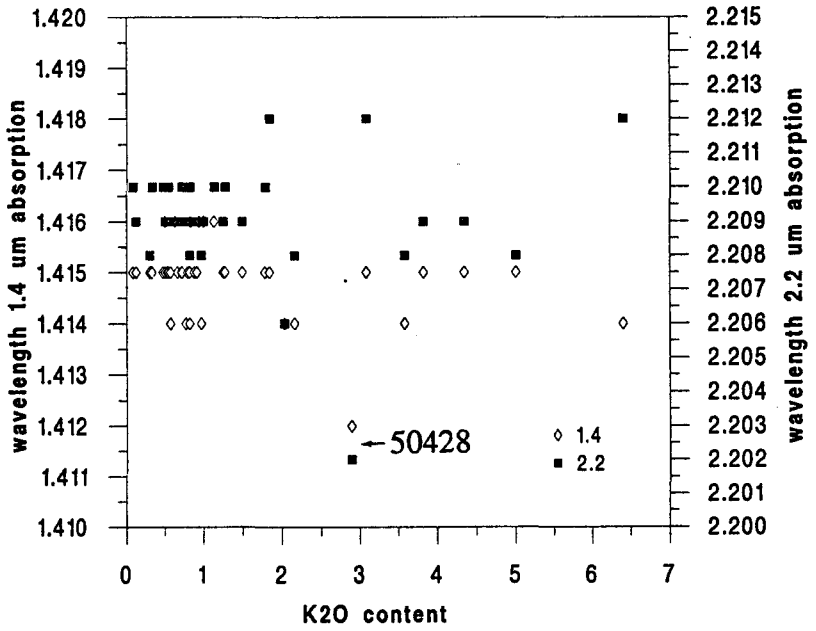


**Figure 4:** A plot of the $K_2O$ content (related to the K-mica abundance) versus the wavelengths of both the 1.4 and 2.2 $\mu$m absorptions for all the samples.

other minerals detected using XRD (chlorite, amphibole, calcite, plagioclase, talc, vermiculite) are not evident in the spectra. The spectra also show absorptions related to gypsum (Figure 3e), mica and possibly alunite (Figure 3d).

The presence of mica in these samples was examined in the spectra using the wavelengths of the OH absorptions at 1.4 and 2.2 $\mu$m. These wavelengths are plotted against the $K_2O$ contents (muscovite abundance) in Figure 4 which shows the 1.4 $\mu$m absorptions are precisely located at 1.415 $\mu$m and the 2.2 $\mu$m absorptions are precisely located at 2.209 $\mu$m. These wavelengths are approximately 10 nm longer than those expected for muscovite and paragonite (Section 6.0). These longer wavelengths, if significant, may be caused by the presence of other clays, such as kaolinite. This explanation is consistent with the kaolinite-poor, muscovite-rich sample (50428, Appendix 1.1) showing the shortest wavelengths to the 1.4 and 2.2 $\mu$m absorptions (labelled in Figure 4). The data in Figure 4 also show no relationship between the $K_2O$ content and the wavelengths of the 1.4 and 2.2 $\mu$m absorptions, indicating that changes in the muscovite content ($K_2O$ content) do not significantly affect the wavelengths of these absorptions.

The presence of mica (K-rich and/or Na-rich) was examined using the 2.35 $\mu$m absorption (Section 6.0). The presence of this absorption was first tested using a technique available in PCSpectra, called "Feature Extraction", which filters hull quotient spectra for absorption features deeper than a nominated "noise level" (noise level was selected as 0.015 of the hull quotient depth). The results from this analysis (Appendix 1) show the 2.35 $\mu$m absorption is present in only a handful of spectra even though the majority of samples contained mica as shown by the XRD results. This suggests a "threshold" mica content is required in a material before the 2.35 $\mu$m absorption becomes apparent in reflectance data.

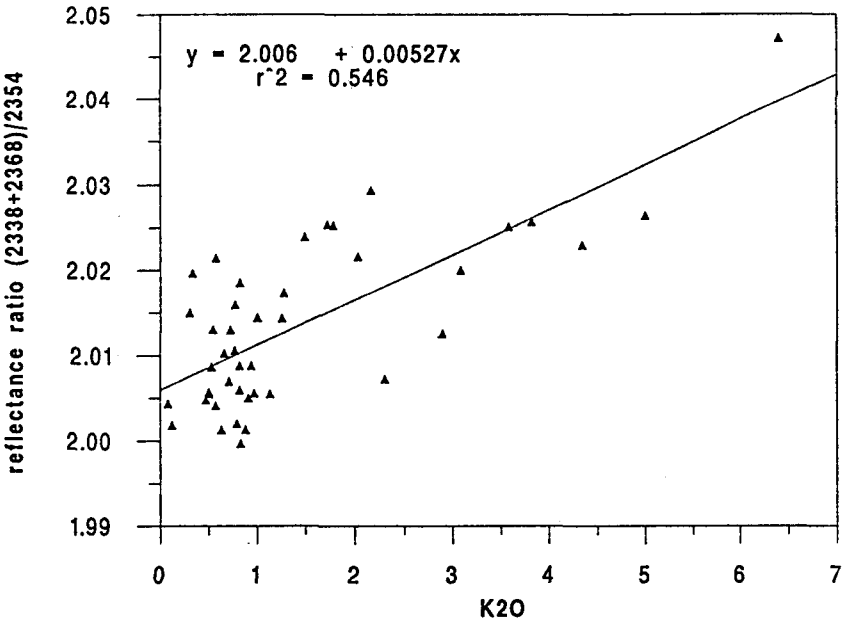


**Figure 5:** A plot of the $K_2O$ content (related to the K-mica abundance) versus the depth of the 2.35 $\mu$m absorption (calculated using a ratio of reflectances described in Section 8.0) for all samples.

The depth of the 2.35 $\mu$m absorption was also calculated using a sum of the reflectances taken from the edges of this absorption (2.338 and 2.368 $\mu$m) divided by the reflectance of the absorption minima (2.354 $\mu$m). The results of this ratio are plotted against the $K_2O$ contents in Figure 5 which shows significant correlation. This confirms the original assumption that K is largely contained in K-bearing micas (muscovite, illite). The hull quotient results (Appendix 1) and the ratio results (Figure 5) show the minimum $K_2O$ content required to produce the 2.35 $\mu$m absorption is approximately 3%. The 3% $K_2O$ equates to approximately 20% (by weight) of muscovite or 30% (by weight) of illite.

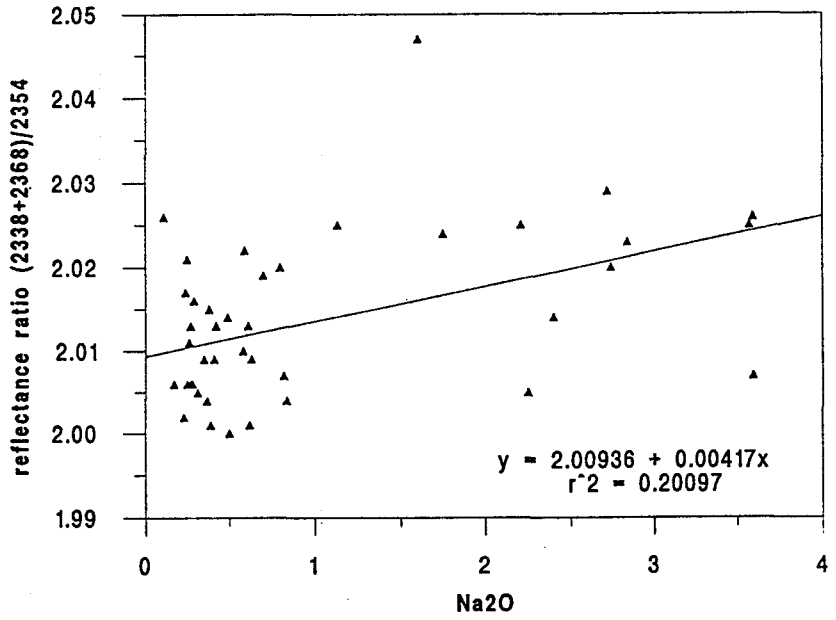


**Figure 6:** A plot of the $Na_2O$ content versus the depth of the 2.35 $\mu$m absorption (calculated using a ratio of reflectances described in Section 8.0) for all samples.

A similar analysis between the 2.35 $\mu$m reflectance ratio and the $Na_2O$ content (Figure 6) showed poor correlation, suggesting that $Na^+$ is not exclusively contained in Na-bearing mica (paragonite, brammallite).

## 8.1 Drill Core

The drill core spectra (Appendix 1.1) were examined because they represent the best examples of muscovite-rich and paragonite-rich materials from the study area. Therefore, they should provide the best data for establishing spectral discrimination of these micas. This suite of samples also contained Na-muscovite, illite and brammallite (Na-equivalent of illite) determined from electron microprobe analyses of the interlayer and octahedral cations (Appendix 3).

The drill core spectra included muscovite-rich samples (39223, 39235 and 50420) and paragonite-rich samples (39131 and 39153). Most of the muscovite-rich samples contain approximately 3% $K_2O$ and show development of the 2.35 $\mu$m absorption. The paragonite-rich samples contain approximately 2% $Na_2O$ but show no development of the 2.35 $\mu$m absorption. This result, combined with the lack of change in the wavelengths of the 1.4 and 2.2 $\mu$m absorptions (Section 8.0), indicates there are no differences between the muscovite-rich and paragonite-rich spectra, except one of total mica abundance (depth of the 2.35 $\mu$m absorption), which is not considered to be diagnostic. Therefore, the species of mica in these samples cannot be discriminated using these reflectance properties.

## 8.2 Subcrop

The subcrop spectra were examined to determine the variability in spectral behaviour and relationships with host rock. The reflectance spectra of the subcrop samples, together with their associated mineralogy and geochemistry, are presented in Appendix 1.2.

The subcrop spectra show variation in spectral behaviour. Samples 108085, 108087 and 108094 show narrow, single absorptions at 1.4, 2.2 and 2.35 $\mu$m indicating the presence of mica (muscovite, paragonite, sericite, illite). Kaolinite-related absorptions are weak to non-existent in these spectra. These samples are rich in silica (64-93% $SiO_2$), have variable aluminium (4-21% $Al_2O_3$) and are poor in iron (0.3-0.6% $Fe_2O_3$) and magnesium (0.1-0.9% MgO). This composition is indicative of quartz to quartz-feldspathic sediments. At these wavelengths, quartz is relatively transparent to electromagnetic radiation (EMR), such that greater interaction occurs between mica and EMR producing better muscovite/illite absorptions. This could explain why the silica-rich sample 108110 (93% $SiO_2$) with $<1.0\%$ $K_2O$, has well developed absorption at 2.35 $\mu$m.

The spectra of samples 108090a, 108092a 108092b and 108110 are characterised by well developed kaolinite absorptions at 1.360, 1.400, 2.165, 2.196, 2.320 and 2.384 (Figure 3g) (characteristic of saprolite; Cudahy, 1992a). This suite of samples are rich in aluminium (9-30% $Al_2O_3$), variable in iron (1-52% $Fe_2O_3$) and silica (27-64%) and poor in magnesium (0.2-1.0% MgO). The $K_2O$ contents of these samples are variable. For

example, sample 108110 contains 3.82% $K_2O$ and its spectra shows mica absorption at 2.35 $\mu$m, whereas, sample 108092a contains 0.08% $K_2O$, and its spectra shows no evidence for the 2.35 $\mu$m absorption. Geological and geochemical evidence suggests that these samples are weathered, mafic volcanic rocks of saprolite/mottled zone (Lintern and Scott, 1990; Cudahy, 1992a). If this interpretation is correct, then mica-bearing mafic rocks from the upper parts of the laterite profile contain mica minerals in sufficient abundance to cause recognisable absorption at 2.35 $\mu$m. This has major implications for spectral sensing applications (Section 8.4).

## 8.3 Soil

The soil spectra were examined because, if mica-related absorptions are found to be evident in these spectra, then remote sensing techniques could be used to map the surface distribution of mica. The soil reflectance spectra and the associated mineralogical and geochemical data are presented in Appendix 1.3.

The soil reflectance spectra show consistent information characterised by asymmetric OH-related absorptions with minima at 1.415 and 2.209 $\mu$m, deep water absorption at 1.916 $\mu$m and a small absorption at 2.25 $\mu$m. These spectral characteristics are similar to the spectra of soils from the Laverton region (Cudahy, 1992b) and the Beasley Creek gold deposit (Cudahy and others, 1992a) and are indicative of poorly crystalline kaolinite (Cudahy, 1992a). There is no clear development of the mica-absorption at 2.35 $\mu$m. This is consistent with the relatively low $K_2O$ abundances of these soils ($<1.0\%$).

## 8.4 Implications for Gold Exploration

The results show two restrictions for the mapping and discrimination of micas in the Yilgarn Craton using spectral techniques. Firstly, the reflectance data provided no evidence for the discrimination of the micas; muscovite and paragonite. Secondly, the mica-related absorption at 2.35 $\mu$m becomes apparent only when more than 20% (by weight) of mica is contained in the sample. Some of the subcrop and drill core samples contained sufficient abundance of mica to develop the 2.35 $\mu$m absorption. However, the soils did not have sufficient abundance of mica. Therefore, remote sensing strategies are restricted by the availability, at the surface, of mica-bearing, mafic rock. If soils dominate the surface materials, as is the case at Panglo, Mt Hope (Cudahy and others, 1992b) and Beasley Creek (Cudahy and others, 1992a), then it will not be possible to remotely detect K-micas unless the soils are dominated by quartz. Soils with $<1.0\%$ $K_2O$ formed from quartz-rich felsic rocks can produce the K-mica absorption at 2.35 $\mu$m (Cudahy, 1992b) though these K-micas are not necessarily related to gold mineralisation. Therefore, it is also important to establish the composition of the parent rocks before deciding the significance of mica-related absorption.

Proximal sensing strategies are better suited to the mapping of mica, though further work is required on determining whether different mica species (both K-rich and K-poor) can be discriminated. Samples of subcrop and/or drill core could be measured in the field using a spectrometer, such as the PIMA-II.

In the context of regolith mapping for geochemical exploration, the limited data show an interesting relationship between weathered mafic subcrop and well-crystalline kaolinite. Further work is required to determine if this is a more general and diagnostic relationship. If this relationship was found to be correct, then a material showing the 2.35 $\mu$m absorption and well-developed absorption doublets at 1.4 and 2.2 $\mu$m could be interpreted as mica-bearing, weathered mafic rock potentially associated with gold mineralisation.

## 9.0 CONCLUSIONS

The high-spectral resolution PIMA-II spectrometer was used to measure the 1.3 to 2.5 $\mu$m reflectance spectra of muscovite- and paragonite-bearing weathered materials associated with gold mineralisation at Panglo, Western Australia. These minerals were of particular interest as gold mineralisation in the Yilgarn Craton is commonly associated with potassic alteration indicated by the development of K-bearing phyllosilicates.

The reflectance spectra show:

1. The wavelengths of the 1.4 or 2.2 $\mu$m absorptions are not specifically related to muscovite or paragonite;

2. The $K_2O$ content (related to the muscovite/illite content) can be correlated with the depth of mica-related absorption at 2.35 $\mu$m. No equivalent relationship was established for the $Na_2O$ content and the 2.35 $\mu$m absorption, probably because of complications associated with halite;

3. In quartz-poor materials ($<60\%$ $SiO_2$), $>3\%$ $K_2O$ is required in a sample before the 2.35 $\mu$m absorption becomes apparent in reflectance spectra;

4. Mica-bearing, weathered mafic volcanics possess well developed kaolinite absorptions at 1.395, 1.415, 2.165 and 2.209 $\mu$m in addition to mica-related absorption at 2.35 $\mu$m. Mica-bearing shales showed poor development of kaolinite absorptions; and

5. The soil spectra are characterised by poorly crystalline kaolinite absorptions but no evidence for mica-related absorption at 2.35 $\mu$m which is related to their low $K_2O$ contents of less than 1%.

These results suggest remote sensing for potassic micas will be difficult in soil-dominated mafic terrains. However, there may be some opportunity in areas of substantial outcrop (if they exist) or in quartz-rich, residual soils. Field-based applications that require information on the detection and abundance of K-bearing micas are better suited to the results of this study.

## 10.0 FURTHER WORK

Further work is required on determining the relationships between spectral properties and mineralogical and geochemical information, including:

1. Establishing the spectral characteristics and detection limits for paragonite/brammallite, fuchsite and other micas/clays;

2. Determining the affects of replacement in the mica lattice by $Fe^{2+}$, $Si^{4+}$, $Mg^{2+}$ and other elements; and

3. Establishing if associations exist between spectral properties and geological/regolith units (rock type, alteration and weathering), in particular, whether well-crystalline kaolinite is diagnostic of weathered mafic rock.;

## 11. ACKNOWLEDGEMENTS

This study has been financially supported by industry and government sponsorship of the AMIRA/CSIRO P243 Remote Sensing for Gold Project in W.A.. Pancontinental Mining provided permission to work with their samples from the Panglo area. Jon Huntington organised the measurement of the samples at the North Ryde laboratories using the PIMA-II. To all these we express our sincere thanks.

## 12.0 REFERENCES

**BUCKINGHAM, W. F. and SOMMER, S. E., 1983.** Mineralogical characterisation of rock surfaces formed by hydrothermal alteration and weathering - application to remote sensing. Economic Geology, Vol. 78, pp. 664-674.

**BUTT, C. R. M. 1991.,** Dispersion of gold and associated elements in the lateritic regolith, Mystery Zone, Mt Percy, Kalgoorlie, Western Australia. CSIRO, IMEC, Division of Exploration Geoscience Restricted Investigation Report No. 156R, .

**BUTT, C. R. M., GRAY, D. J., LINTERN, M. J., ROBERTSON, I. D. M., TAYLOR, G. F. and SCOTT, K. M., 1991.** Gold and associated elements in the regolith - dispersion processes and implications for exploration - Final Report. CSIRO Division of Exploration Geoscience Restricted Investigation Report No. 167R.

**CLARK, M. E., CARMICHAEL, D. M. and HODGSON. C.J., 1988.,** Metasomatic processes and T-$CO_2$ conditions of wall rock alteration, Victory Gold Mine, Kambalda, Western Australia. Bicentennial Gold 88, Melbourne, May, pp. 230-234.

**CLARK, R. N., TRUDE, V. V., KLEJWA, M., SWAYZE, G. A., and VERGO, N., 1990.** High spectral resolution reflectance spectroscopy of minerals. Journal of Geophysical Research, Vol. 95, No. B8, pp. 12653-12680.

**CUDAHY, T. J., 1992a.** A model for the development of the regolith of the Yilgarn Craton incorporating selected spectral information. CSIRO, IMEC, Division of Exploration Geoscience Restricted Investigation Report No. 243R, 35 pages.

**CUDAHY, T. J., 1992b.** Spectral properties of rocks and soils from the Laverton region, Western Australia. CSIRO, IMEC, Division of Exploration Geoscience Restricted Investigation Report No. 235R, 65 pages.

**CUDAHY, T. J., ROBERTSON, I. D. M., and GABELL, A. R., 1992a.** Spectral properties of the soils and lags overlying the site of the Beasley Creek gold mine, Laverton, Western Australia. CSIRO, IMEC, Division of Exploration Geoscience Restricted Investigation Report No. 160R, 40 pages.

**CUDAHY, T. J., LINTERN, M. J., and GABELL, A. R., 1992b.** Spectral properties of the soils overlying the site of the Bounty gold mine, Forrestania region, Western Australia. CSIRO Division of Exploration Geoscience Restricted Investigation Report No. 169R, 40 pages.

**DEER, W. A., HOWIE, R. A. and ZUSSMAN, J., 1977.** An introduction to the rock forming minerals. Longman, London.

**GOZZARD, J. R. and TAPLEY, I. J., 1992.** Regolith-landform mapping in the Lawlers district, Report 2: Terrain classification mapping. CSIRO, IMEC, Division of Exploration Geoscience Restricted Investigation Report No. 240R, 96 pages.

**GREEN, A. A. and CRAIG, M. D., 1985.** Analysis of aircraft spectrometer data with logarithmic residuals. Proceedings of the AIS workshop, Pasadena, NASA, JPL Publication 85-41.

**GROVES, D. I., PHILLIPS, G. N., HO, S. E. and HOUSTON, S. M., 1985.** The nature, genesis and regional controls of gold mineralisation in Archaean greenstone belts of the Western Australian shield: A brief review. Transactions of the Geological Society of South Africa. Vol. 88, pp 135-148.

**HUNT, G. R. and ASHLEY, R. P., 1979.** Spectra of altered rocks in the visible and near infrared. Economic Geology, Vol. 74, pp 1613-1629.

**HUNT, G. R. and SALISBURY, J. W., 1970.** Visible to near-infrared spectra of minerals and rocks: I Silicate Minerals. Modern Geology, Vol. 1, pp 283-300.

**LINTERN, M. J. and SCOTT, K. M., 1991.** The distribution of gold and other elements in soils and vegetation at Panglo, Western Australia. CSIRO, IMEC, Division of Exploration Geoscience Restricted Investigation Report No. 129R.

**PROST, R. and LAPERCHE, V., 1990.** Far infrared study of potassium in micas. Clays and Clay Minerals. Vol. 38, No. 4, pp 351-355.

**ROBERTSON, I. D. M., CHAFFEE, M. A. and TAYLOR, G. F., 1990.** The petrography, mineralogy and geochemistry of a felsic, mafic, ultramafic and metasedimentary weathered profile at Rand Pit, Reedy Mine - Cue, W.A. CSIRO, IMEC, Division of Exploration Geoscience Restricted Investigation Report No. 102R.

**ROSENQUIST, I. T. and JORGENSEN, P., 1963.** Replacement in the octahedral and interlayer positions in micas. Nature, Vol. 197, No. 4866, pp477-478.

**SCOTT, K. M., 1990.** The mineralogical and geochemical effects of weathering on volcanics from the Panglo deposit, Eastern Goldfields, W.A.. CSIRO, IMEC, Division of Exploration Geoscience Restricted Investigation Report No. 143R.

**SCOTT, K. M. and DOTTER, L. E., 1990.** The mineralogical and geochemical effects of weathering on shales at the Panglo deposit, Eastern Goldfields, W.A. CSIRO, IMEC, Division of Exploration Geoscience Restricted Investigation Report No. 171R.

**SCOTT, K. M. and MARTINEZ, A., 1990.** The mineralogical and geochemical effects of weathering in mafic and ultramafic profiles, Mt Magnet, W.A.. CSIRO, IMEC, Division of Exploration Geoscience Restricted Investigation Report No. 178R.

**VEDDER, W., 1964.** Correlations between infrared spectrum and chemical composition of micas. The American Mineralogist. Vol. 49, pp 736-766.

**VEDDER, W. and McDONALD, R. S., 1962.** Vibrations of the OH ions in muscovite. The Journal of Chemical Physics. Vol. 38, No. 7, pp 1583-1590.

**WHITE, J. L., BAILEY, G. W., BROWN, C. B. and ALRICHS, J. L., 1961.** Infrared investigation of the migration of lithium ions into empty octahedral sites of muscovite and montmorillonite. Nature, Vol. 190, pp 342.

# APPENDICES

## Appendix 1.1

PIMA-II reflectance spectra and associated mineralogical
and geochemical data for the drill core samples. No iron oxide information is presented.

**29635**

Muscovite-rich Shale

6500mN
PSRC 172: 5-6m

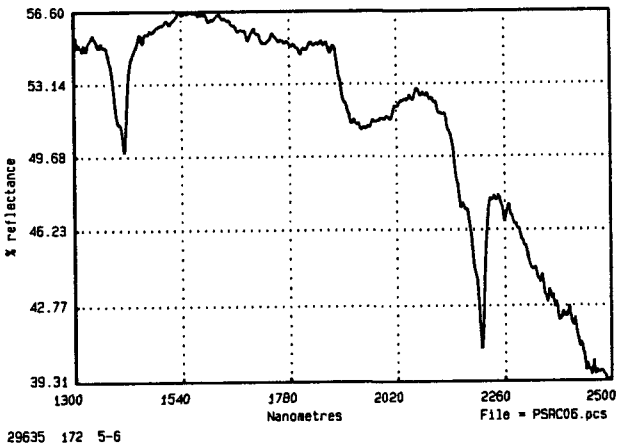


2.35 μm Absorption
0.034 HQ

Oxide abundances

| | |
|---|---|
| $SiO_2$ | 52.8% |
| $Al_2O_3$ | 13.8% |
| $Fe_2O_3$ | 20.5% |
| MgO | 0.39% |
| CaO | <0.04% |
| $Na_2O$ | 1.13% |
| $K_2O$ | 1.78% |
| Au | 0.96 ppm |

Mineral Abundances

| | |
|---|---|
| quartz | 6 |
| muscovite | 6 |
| kaolinite | 6 |
| halite | 4 |
| alunite | 2 |
| halite | |

**39131**

Paragonite-rich Mafic
(brammallite)

PSRC 238: 27-28m

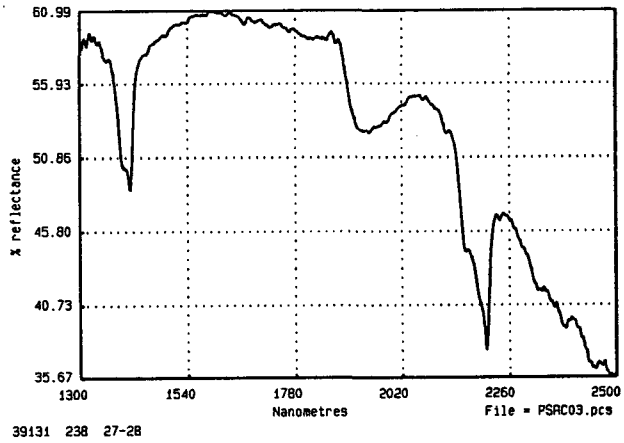


2.35 μm absorption
nil

Oxide Abundances

| | |
|---|---|
| $SiO_2$ | 37.6% |
| $Al_2O_3$ | 26.3% |
| $Fe_2O_3$ | 19.2% |
| MgO | 0.30% |
| CaO | <0.04% |
| $Na_2O$ | 2.40% |
| $K_2O$ | 1.25% |
| Au | 0.01ppm |

Mineral Abundances

| | |
|---|---|
| kaolinite | 6 |
| quartz | 6 |
| para./musc. | 6 |
| halite | 6 |
| Na-illite | |

**39153**

Paragonite-rich Mafic
(muscovite)

PSRC 238: 48-49m

2.35 μm absorption
nil

Oxide Abundances

| | |
|---|---|
| $SiO_2$ | 56.8% |
| $Al_2O_3$ | 18.8% |
| $Fe_2O_3$ | 13.1% |
| MgO | 0.31% |
| CaO | <0.04% |
| $Na_2O$ | 1.75% |
| $K_2O$ | 1.49% |
| Au | 0.01 ppm |

Mineral Abundances

| | |
|---|---|
| kaolinite | 6 |
| quartz | 6 |
| mus./para. | 6 |
| halite | 4 |
| smectite | 2 |

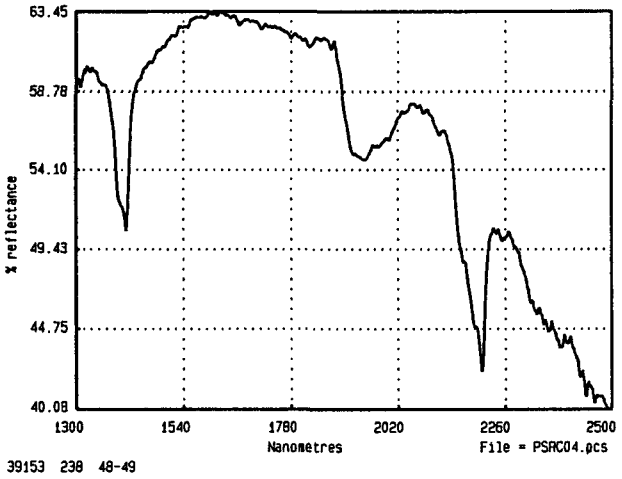


**39223**

Muscovite-rich Mafic

PSRC 239: 46-47m

2.35 μm Absorption
0.034 HQ

Oxide Abundances

| | |
|---|---|
| $SiO_2$ | 49.9% |
| $Al_2O_3$ | 20.8% |
| $Fe_2O_3$ | 11.1% |
| MgO | 0.52% |
| CaO | <0.04% |
| $Na_2O$ | 2.72% |
| $K_2O$ | 2.16% |
| Au | 0.01 ppm |

Mineral Abundances

| | |
|---|---|
| kaolinite | 6 |
| quartz | 6 |
| muscovite | 6 |
| halite | 6 |
| smectite | 1 |

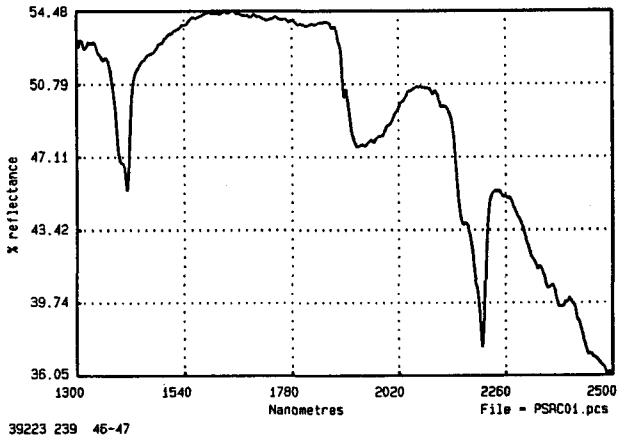

**39235**

Muscovite-rich Mafic

PSRC 239: 56-57m

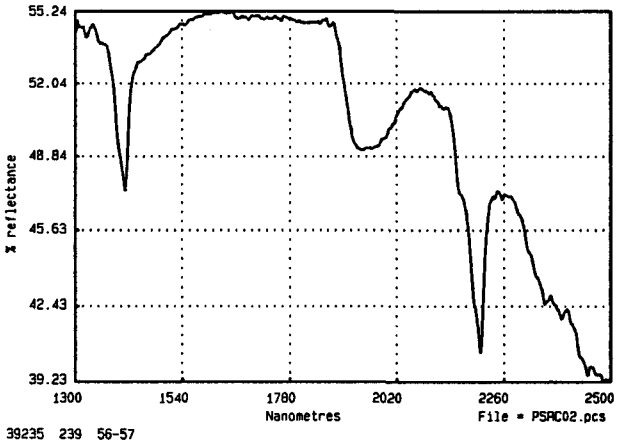


2.35 μm Absorption
0.045 HQ

Oxide Abundances

| | |
|---|---|
| $SiO_2$ | 46.6% |
| $Al_2O_3$ | 21.3% |
| $Fe_2O_3$ | 9.69% |
| MgO | 0.70% |
| CaO | <0.04% |
| $Na_2O$ | 3.57% |
| $K_2O$ | 3.58% |
| Au | 0.01 ppm |

Mineral Abundances

| | |
|---|---|
| kaolinite | 6 |
| quartz | 6 |
| muscovite | 6 |
| halite | 6 |
| smectite | 2 |

**50420**

Muscovite-rich Shale
(illite)

PSRC 341: 6-7m

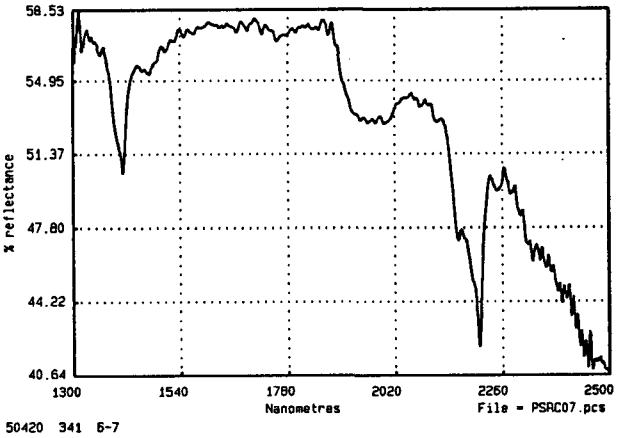


2.35 μm Absorption
nil

Oxide Abundances

| | |
|---|---|
| $SiO_2$ | |
| $Al_2O_3$ | 16.4% |
| $Fe_2O_3$ | 3.19% |
| MgO | 0.52% |
| CaO | 0.05% |
| $Na_2O$ | 1.93% |
| $K_2O$ | 3.07% |
| Au | 0.02 ppm |

Mineral Abundances

| | |
|---|---|
| kaolinite | 6 |
| muscovite | 6 |
| quartz | 6 |
| alunite | 6 |
| halite | 6 |
| talc | 3 |

**50428**

Na-muscovite-rich Shale

PSRC 341: 12-13m

<u>2.35 μm Absorption</u>
0.065HQ

<u>Oxide Abundance</u>

| | |
|---|---|
| Au | 0.01 |

<u>Mineral Abundances</u>

| | |
|---|---|
| quartz | 6 |
| alunite | 6 |
| muscovite | 6 |
| kaolinite | 4 |
| halite | 4 |

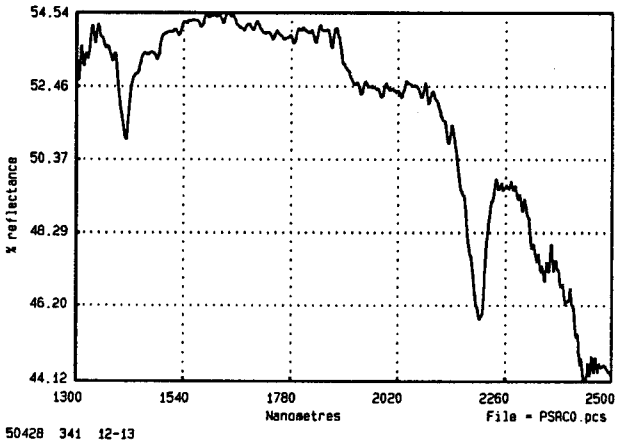

## Appendix 1.2

PIMA-II reflectance spectra and associated mineralogical
and geochemical data for the subcrop samples. No iron oxide data are presented.

**108083**

Shale
2690 mE, 4200 mN

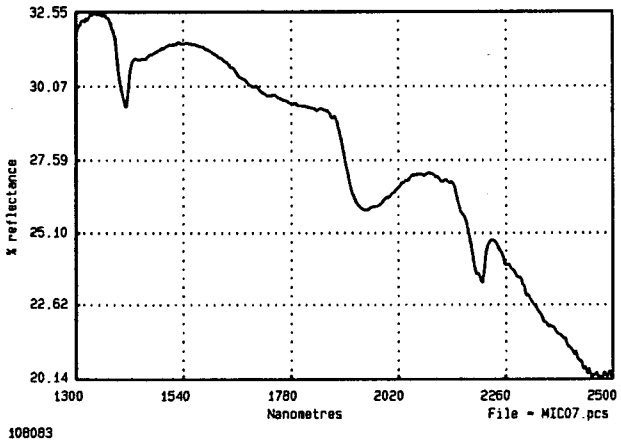


2.35 μm Absorption
0.046 HQ

Oxide Abundance

| | |
|---|---|
| $SiO_2$ | 75.6% |
| $Al_2O_3$ | 5.1% |
| $Fe_2O_3$ | 14.5% |
| MgO | 0.05% |
| CaO | 0.02% |
| $Na_2O$ | 0.38% |
| $K_2O$ | 0.30% |

Mineral Abundance

| | |
|---|---|
| quartz | 6 |
| kaolinite | 4 |
| talc | 4 |
| muscovite | 3 |
| verm./chlor. | 3 |
| halite | 3 |
| smectite | 1 |
| gypsum | |

**108085**

Shale
2675 mE 4200 mN

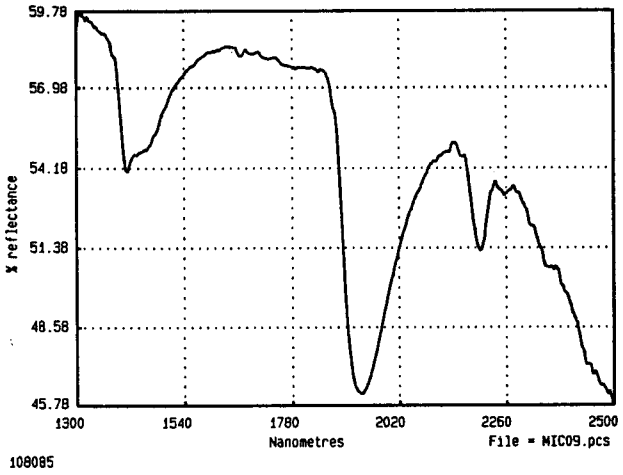


2.35 μm Absorption
0.046 HQ

Oxide Abundance

| | |
|---|---|
| $SiO_2$ | 78.6 |
| $Al_2O_3$ | 11.6 |
| $Fe_2O_3$ | 0.5 |
| MgO | 0.47 |
| CaO | 0.04 |
| $Na_2O$ | 0.61 |
| $K_2O$ | 2.89 |

Mineral Abundance

| | |
|---|---|
| quartz | 6 |
| alunite | 6 |
| muscovite | 5 |
| verm./chlor. | 4 |
| halite | 4 |

**108087**

Shale
2660 mE 4200 mN

2.35 μm Absorption
0.020 HQ

Oxide Abundance

| | |
|---|---|
| $SiO_2$ | 93.4% |
| $Al_2O_3$ | 3.5% |
| $Fe_2O_3$ | 0.3% |
| MgO | 0.11% |
| CaO | 0.06% |
| $Na_2O$ | 0.49% |
| $K_2O$ | 1.00% |

Mineral Abundance

| | |
|---|---|
| quartz | 6 |
| muscovite | 5 |
| halite | 4 |
| vermi/chlorite | 3 |

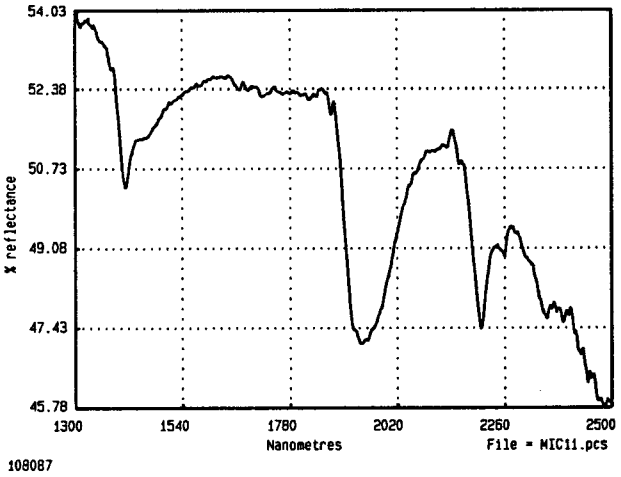


**108090a**

Mafic Volcanic
2645 mE 4200 mN

2.35 μm Absorption
nil

Oxide Abundance

| | |
|---|---|
| $SiO_2$ | 27.3% |
| $Al_2O_3$ | 9.1% |
| $Fe_2O_3$ | 52.1% |
| MgO | 0.23% |
| CaO | 0.07% |
| $Na_2O$ | 0.42% |
| $K_2O$ | 0.54% |

Mineral Abundance

| | |
|---|---|
| quartz | 6 |
| verm./chlor. | 5 |
| talc | 4 |
| muscovite | 3 |
| smectite | 1 |

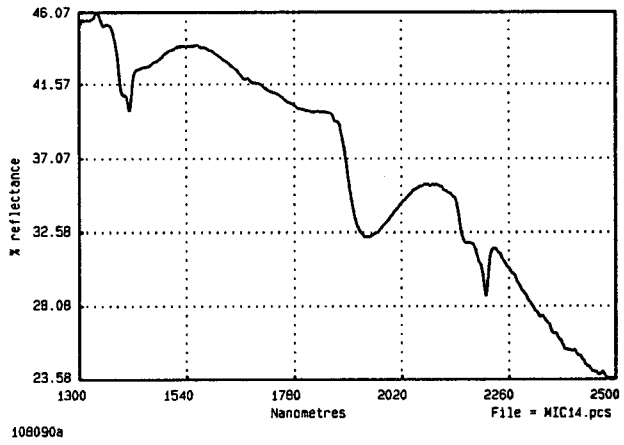

**108092a**

Mafic Volcanic
2630 mE 4200 mN

<u>2.35 μm Absorption</u>
nil

<u>Oxide Abundance</u>

| | |
|---|---|
| $SiO_2$ | 32.0% |
| $Al_2O_3$ | 8.7% |
| $Fe_2O_3$ | 45.6% |
| MgO | 0.25% |
| CaO | 0.02% |
| $Na_2O$ | 0.84% |
| $K_2O$ | 0.08% |

<u>Mineral Abundance</u>

| | |
|---|---|
| quartz | 6 |
| kaolinite | 4 |
| halite | 3 |
| verm./chlor. | 2 |
| talc | 1 |
| gypsum | ? |

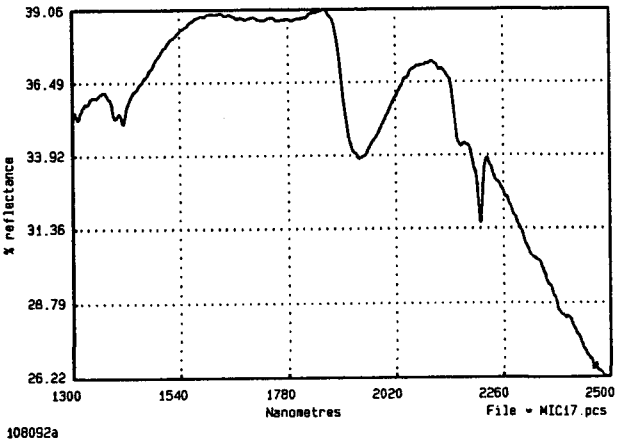


**108092b**

Mafic Volcanic
2630 mE 4200 mN

<u>2.35 μm Absorption</u>
nil

<u>Oxide Abundance</u>

| | |
|---|---|
| $SiO_2$ | 64.3% |
| $Al_2O_3$ | 16.3% |
| $Fe_2O_3$ | 1.2% |
| MgO | 0.80% |
| CaO | 0.11% |
| $Na_2O$ | 2.74% |
| $K_2O$ | 0.33% |

<u>Mineral Abundance</u>

| | |
|---|---|
| quartz | 6 |
| kaolinite | 6 |
| talc | 6 |
| halite | 6 |
| verm./chlor. | 5 |
| smectite | 3 |
| para./musc. | 3 |

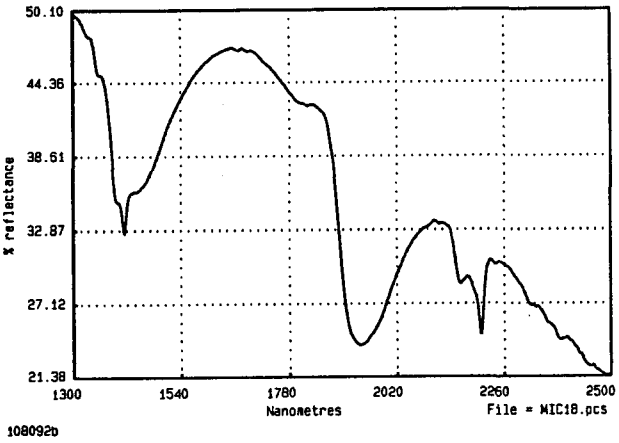

## 108094

Shale
2616 mE 4200 mN

<u>2.35 μm Absorption</u>
0.028 HQ

<u>Oxide Abundance</u>

| | |
|---|---|
| $SiO_2$ | 63.6% |
| $Al_2O_3$ | 20.8% |
| $Fe_2O_3$ | 0.6% |
| MgO | 0.88% |
| CaO | 0.02% |
| $Na_2O$ | 0.11% |
| $K_2O$ | 5.0% |

<u>Mineral Abundance</u>

| | |
|---|---|
| quartz | 6 |
| muscovite | 6 |
| talc | 6 |
| halite | 6 |
| verm./chlor. | 5 |
| gypsum | ? |

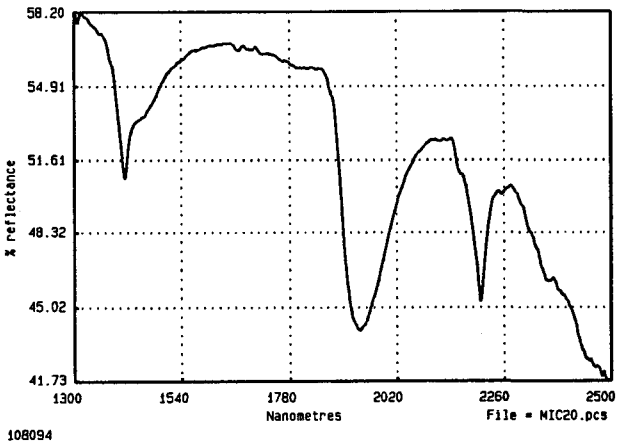


## 108096a

Shale
2600 mE 4200 mN

<u>2.35 μm Absorption</u>
0.035 HQ

<u>Oxide Abundance</u>

| | |
|---|---|
| $SiO_2$ | 48.5% |
| $Al_2O_3$ | 10.7% |
| $Fe_2O_3$ | 25.7% |
| MgO | 0.82% |
| CaO | 0.13% |
| $Na_2O$ | 0.80% |
| $K_2O$ | 3.08% |

<u>Mineral Abundance</u>

| | |
|---|---|
| quartz | 6 |
| verm./chlor. | 6 |
| musc./para. | 4 |
| halite | 3 |
| smectite | 1 |

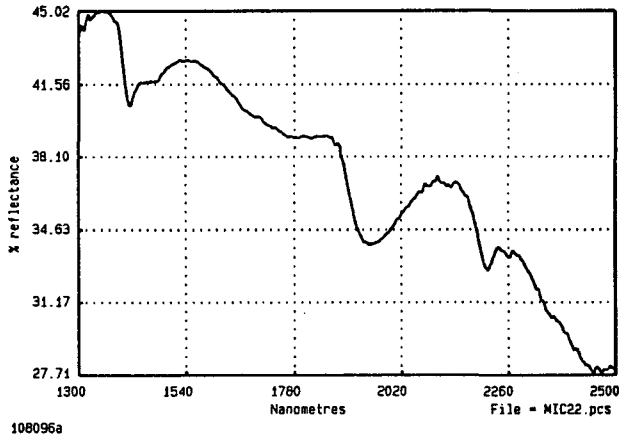

**108096b**

Shale
2600 mE 4200 mN

2.35 μm Absorption
0.102 HQ

Oxide Abundance

| | |
|---|---|
| $SiO_2$ | 57.1% |
| $Al_2O_3$ | 20.9% |
| $Fe_2O_3$ | 2.5% |
| MgO | 1.31% |
| CaO | 0.06% |
| $Na_2O$ | 1.6% |
| $K_2O$ | 6.4% |

Oxide Abundance

| | |
|---|---|
| quartz | 6 |
| muscovite | 6 |
| halite | 6 |
| alunite | 6 |
| verm./chlor. | 2 |

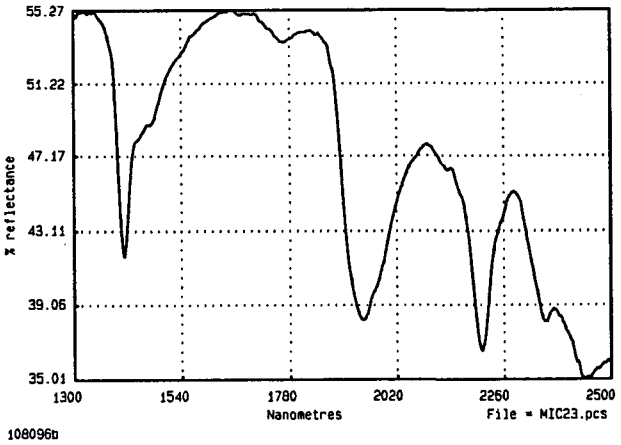


**108098a**

Shale
2587 mE 4200 mN

2.35 μm Absorption
nil

Oxide Abundance

| | |
|---|---|
| $SiO_2$ | 28.9% |
| $Al_2O_3$ | 6.9% |
| $Fe_2O_3$ | 51.8% |
| MgO | 0.32% |
| CaO | 0.02% |
| $Na_2O$ | 0.70% |
| $K_2O$ | 0.82% |

Mineral Abundance

| | |
|---|---|
| quartz | 6 |
| talc | 4 |
| muscovite | 3 |
| kaolinite | 3 |
| verm./chlor. | 2 |
| smectite | 1 |

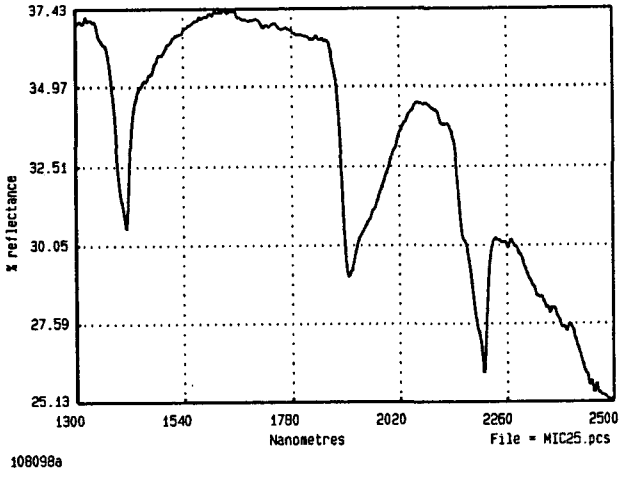

**108098**

Shale
2587 mE 4200 mN

<u>2.35 μm Absorption</u>
nil

<u>Oxide Abundance</u>

| | |
|---|---|
| $SiO_2$ | 28.9% |
| $Al_2O_3$ | 6.9% |
| $Fe_2O_3$ | 51.8% |
| MgO | 0.32% |
| CaO | 0.02% |
| $Na_2O$ | 0.70% |
| $K_2O$ | 0.82% |

<u>Mineral Abundance</u>

| | |
|---|---|
| quartz | 6 |
| talc | 4 |
| muscovite | 3 |
| kaolinite | 3 |
| verm./chlor. | 2 |
| smectite | 1 |

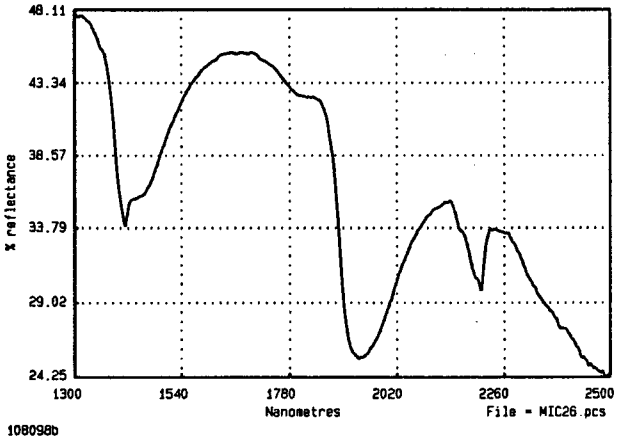


**108101a**

Mafic Volcanic
2560 mE 4200 mN

<u>2.35 μm Absorption</u>
0.052 HQ

<u>Oxide Abundance</u>

| | |
|---|---|
| $SiO_2$ | 19.0% |
| $Al_2O_3$ | 11.8% |
| $Fe_2O_3$ | 54.7% |
| MgO | 0.4% |
| CaO | 0.1% |
| $Na_2O$ | 0.59% |
| $K_2O$ | 2.03% |

<u>Mineral Abundance</u>

| | |
|---|---|
| quartz | 6 |
| muscovite | 5 |
| kaolinite | 4 |
| verm./chlor. | 3 |
| halite | 3 |
| gypsum | 3 |
| talc | 2 |

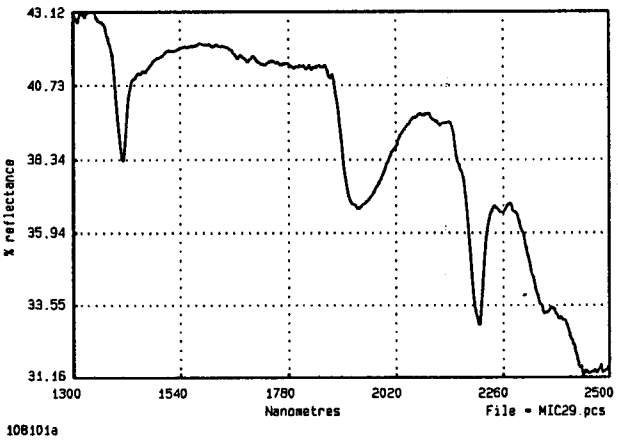

**108101b**

Mafic Volcanic
2560 mE 4200 mN

2.35 μm Absorption
0.040 HQ

Oxide Abundances

| | |
|---|---|
| $SiO_2$ | 45.2% |
| $Al_2O_3$ | 28.8% |
| $Fe_2O_3$ | 2.3% |
| MgO | 0.76% |
| CaO | 0.05% |
| $Na_2O$ | 2.84% |
| $K_2O$ | 4.34% |

Mineral Abundance

| | |
|---|---|
| quartz | 6 |
| muscovite | 6 |
| kaolinite | 6 |
| halite | 6 |
| verm./chlor. | 5 |
| talc | 5 |

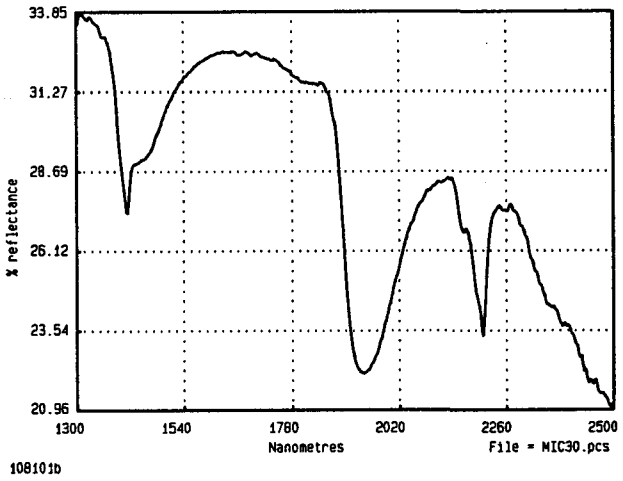


**108102**

Pisoliths

2.35 μm Absorption
nil

Mineral Abundances

| | |
|---|---|
| quartz | 6 |
| kaolinite | 2 |
| muscovite | 3 |
| smectite | 1 |
| talc | 1 |

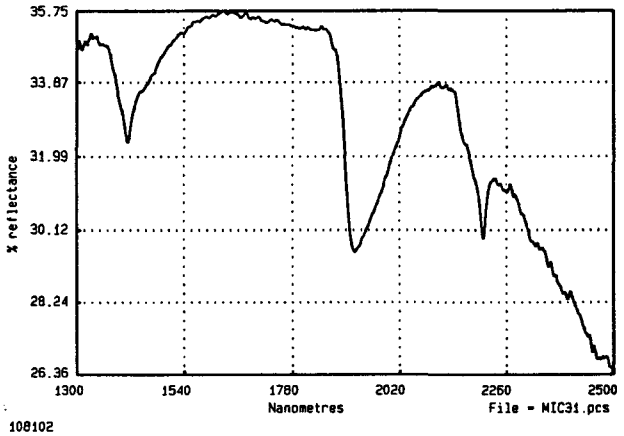

**108103**

Mafic Volcanic
2555 mE 4200 mN

2.35 μm Absorption
nil

Oxide Abundances

| | |
|---|---|
| $SiO_2$ | 9.3% |
| $Al_2O_3$ | 7.0% |
| $Fe_2O_3$ | 69.3% |
| MgO | 0.33% |
| CaO | 0.08% |
| $Na_2O$ | 0.24% |
| $K_2O$ | 1.27% |

Mineral Abundances

| | |
|---|---|
| quartz | 6 |
| talc | 6 |
| verm./chlor. | 5 |
| muscovite | 4 |

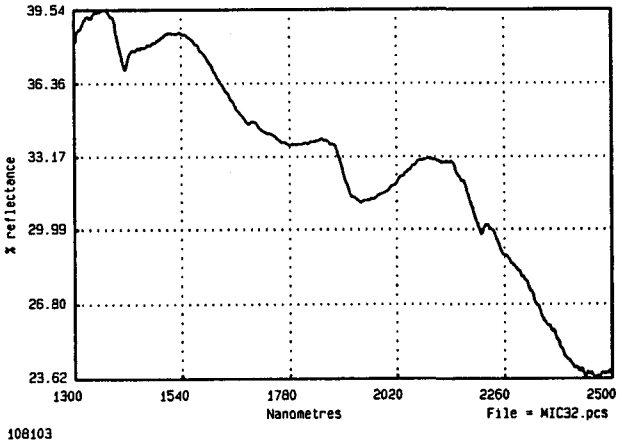


**108107a**

Mafic Volcanic
2520 mE 4200 mN

2.35 μm Absorption
nil

Oxide Abundances

| | |
|---|---|
| $SiO_2$ | 9.5% |
| $Al_2O_3$ | 3.9% |
| $Fe_2O_3$ | 73.1% |
| MgO | 0.53% |
| CaO | 0.08% |
| $Na_2O$ | 0.23% |
| $K_2O$ | 0.12% |

Mineral Abundance

| | |
|---|---|
| quartz | 6 |
| talc | 6 |
| muscovite | 5 |
| verm./chlor. | 5 |
| kaolinite | 4 |
| smectite | 2 |

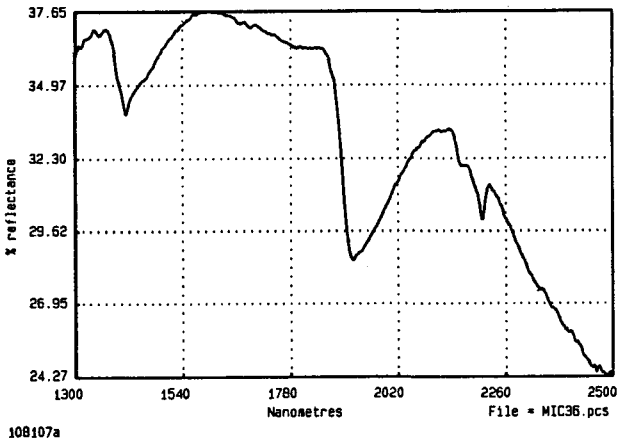

**108107b**

Mafic Volcanic
2520 mE 4200 mN

2.35 μm Absorption
nil

Oxide Abundances

| | |
|---|---|
| $SiO_2$ | 30.4% |
| $Al_2O_3$ | 9.9% |
| $Fe_2O_3$ | 2.1% |
| MgO | 1.85% |
| CaO | 16.3% |
| $Na_2O$ | 0.24% |
| $K_2O$ | 1.84% |

Mineral Abundances

| | |
|---|---|
| quartz | 6 |
| muscovite | 6 |
| gypsum | 6 |
| smectite | 6 |
| kaolinite | 4 |
| talc | 3 |

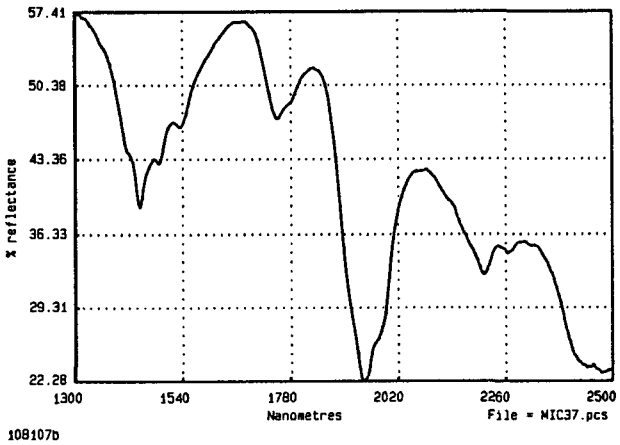


**108110**

Mafic Volcanic
2460 mE 4200 mN

2.35 μm Absorption
0.043 HQ

Oxide Abundance

| | |
|---|---|
| $SiO_2$ | 39.9% |
| $Al_2O_3$ | 30.0% |
| $Fe_2O_3$ | 3.1% |
| MgO | 1.19% |
| CaO | 0.39% |
| $Na_2O$ | 3.59% |
| $K_2O$ | 3.82% |

Mineral Abundance

| | |
|---|---|
| quartz | 6 |
| muscovite | 6 |
| halite | 6 |
| talc | 4 |
| gypsum | 4 |
| verm./chlor. | 3 |
| smectite | 1 |

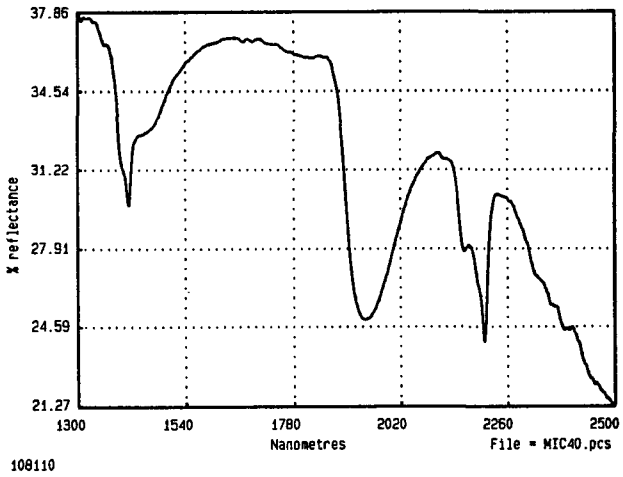

## Appendix 1.3

PIMA-II reflectance spectra and associated mineralogical
and geochemical data for the soil samples. No iron oxide data are presented.

**108077**

2390 mE 3900 mN

<u>2.35 μm Absorption</u>
nil

<u>Mineral Abundance</u>

| | |
|---|---|
| quartz | 6 |
| plagioclase | 6 |
| calcite | 6 |
| kaolinite | 4 |
| muscovite | 2 |
| smectite | 2 |
| talc | 1 |

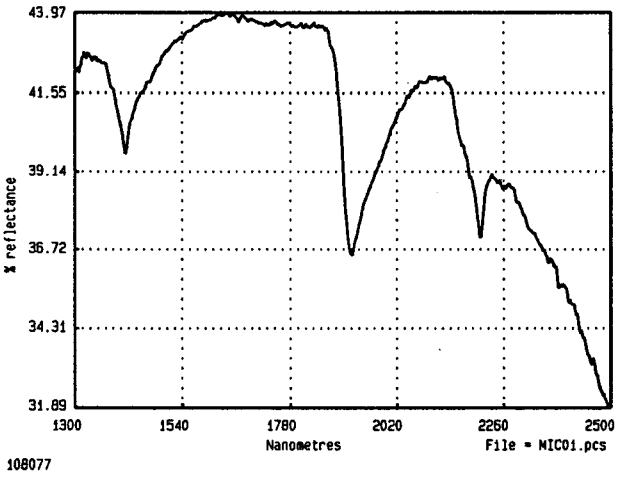


**108078**

2775 mE 4200 mN

<u>2.35 μm Absorption</u>
nil

<u>Oxide Abundance</u>

| | |
|---|---|
| $SiO_2$ | 52.2% |
| $Al_2O_3$ | 14.8% |
| $Fe_2O_3$ | 8.8% |
| MgO | 4.97% |
| CaO | 2.16% |
| $Na_2O$ | 0.28% |
| $K_2O$ | 1.13% |

<u>Mineral Abundances</u>

| | |
|---|---|
| quartz | 6 |
| verm./chlor. | 6 |
| kaolinite | 6 |
| talc | 6 |
| calcite | 5 |
| muscovite | 5 |
| plagioclase | 4 |
| smectite | 1 |

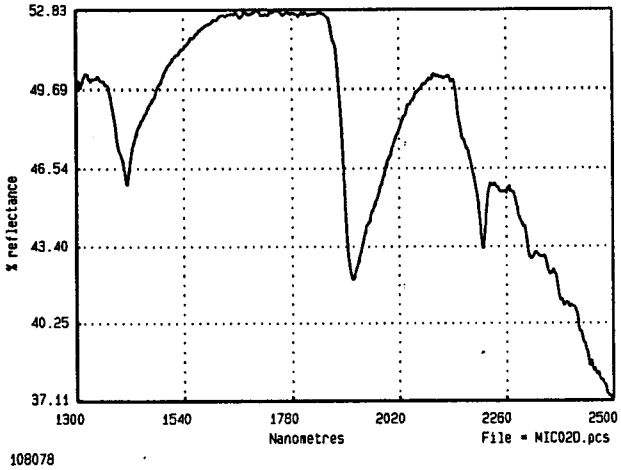

**108079**

2750 mE 4200 mN

<u>2.35 μm Absorption</u>
nil

<u>Oxide Abundance</u>

| | |
|---|---|
| $SiO_2$ | 64.0% |
| $Al_2O_3$ | 11.2% |
| $Fe_2O_3$ | 9.8% |
| MgO | 3.19% |
| CaO | 0.98% |
| $Na_2O$ | 0.23% |
| $K_2O$ | 0.79% |

<u>Mineral Abundance</u>

| | |
|---|---|
| quartz | 6 |
| kaolinite | 5 |
| talc | 5 |
| calcite | 3 |
| muscovite | 3 |
| smecite | 3 |

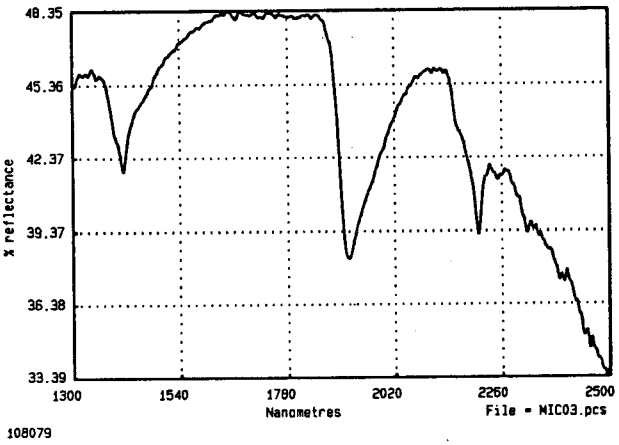


**108080**

2730 mE 4200 mN

<u>2.35 μm Absorption</u>
nil

<u>Oxide Abundance</u>

| | |
|---|---|
| $SiO_2$ | 69.1% |
| $Al_2O_3$ | 10.1% |
| $Fe_2O_3$ | 8.7% |
| MgO | 1.73% |
| CaO | 0.49% |
| $Na_2O$ | 0.31% |
| $K_2O$ | 0.91% |

<u>Mineral Abundance</u>

| | |
|---|---|
| quartz | 6 |
| plagioclase | 6 |
| kaolinite | 5 |
| talc | 5 |
| muscovite | 5 |
| calcite | 3 |
| verm./chlor. | 3 |

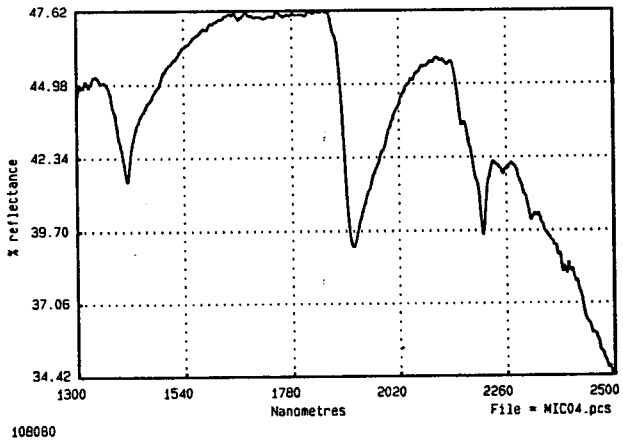

**108081**

2710 mE 4200 mN

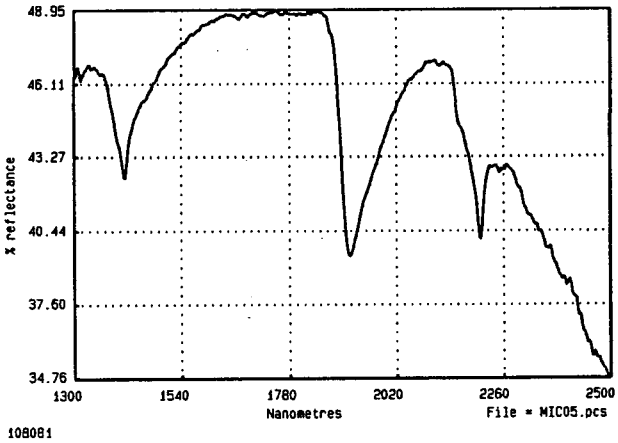


2.35 μm Absorption
nil

Oxide Abundance

| | |
|---|---|
| $SiO_2$ | 72.0% |
| $Al_2O_3$ | 8.4% |
| $Fe_2O_3$ | 10.3% |
| MgO | 1.14% |
| CaO | 0.63% |
| $Na_2O$ | 0.27% |
| $K_2O$ | 0.72% |

Mineral Abundance

| | |
|---|---|
| quartz | 6 |
| kaolinite | 4 |
| plagioclase | 3 |
| calcite | 3 |
| talc | 3 |
| muscovite | 2 |

**108082**

2690 mE 4200 mN

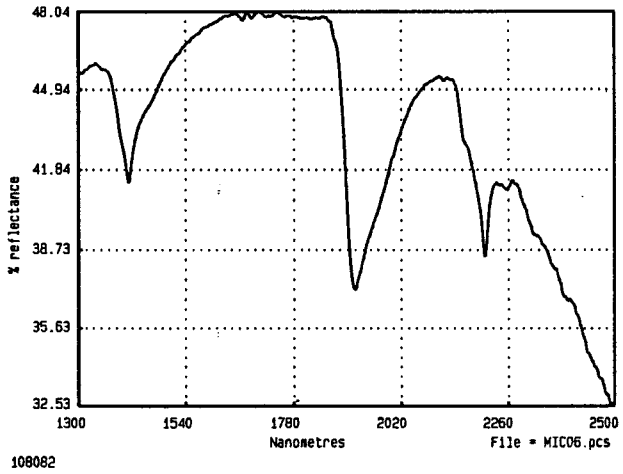


2.35 μm Absorption
nil

Oxide Abundance

| | |
|---|---|
| $SiO_2$ | 66.6% |
| $Al_2O_3$ | 10.9% |
| $Fe_2O_3$ | 9.2% |
| MgO | 1.7% |
| CaO | 0.95% |
| $Na_2O$ | 0.41% |
| $K_2O$ | 0.82% |

Mineral Abundance

| | |
|---|---|
| quartz | 6 |
| kaolinite | 4 |
| calcite | 3 |
| muscovite | 3 |
| smectite | 3 |
| plagioclase | 2 |
| verm./chlor. | 2 |
| talc | 2 |

**108084**

2675 mE 4200 mN

<u>2.35 μm Absorption</u>
nil

<u>Oxide Abundance</u>

| | |
|---|---|
| $SiO_2$ | 68.4% |
| $Al_2O_3$ | 8.0% |
| $Fe_2O_3$ | 13.6% |
| MgO | 1.17% |
| CaO | 0.78% |
| $Na_2O$ | 0.25% |
| $K_2O$ | 0.57% |

<u>Mineral Abundance</u>

| | |
|---|---|
| quartz | 6 |
| plagioclase | 4 |
| kaolinite | 4 |
| calcite | 3 |
| talc | 2 |
| musc./para. | 1 |
| verm./chlor. | 1 |
| paragonite | |

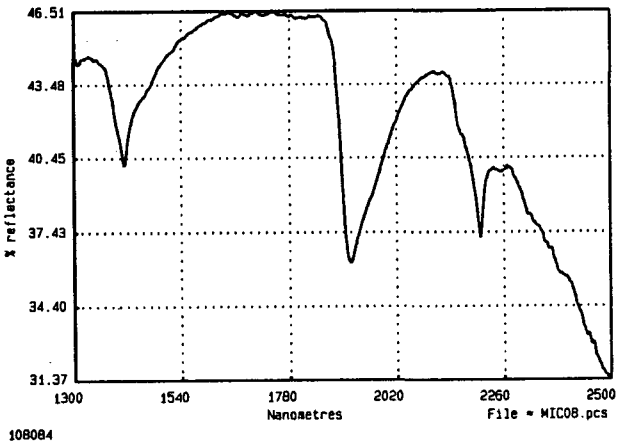


**108086**

2660 mE 4200 mN

<u>2.35 μm Absorption</u>
nil

<u>Oxide Abundance</u>

| | |
|---|---|
| $SiO_2$ | 66.7% |
| $Al_2O_3$ | 10.2% |
| $Fe_2O_3$ | 8.8% |
| MgO | 1.92% |
| CaO | 1.83% |
| $Na_2O$ | 0.26% |
| $K_2O$ | 0.77% |

<u>Mineral Abundance</u>

| | |
|---|---|
| quartz | 6 |
| calcite | 5 |
| kaolinite | 5 |
| smectite | 4 |
| musc./para. | 4 |
| talc | 4 |
| plagioclase | 3 |

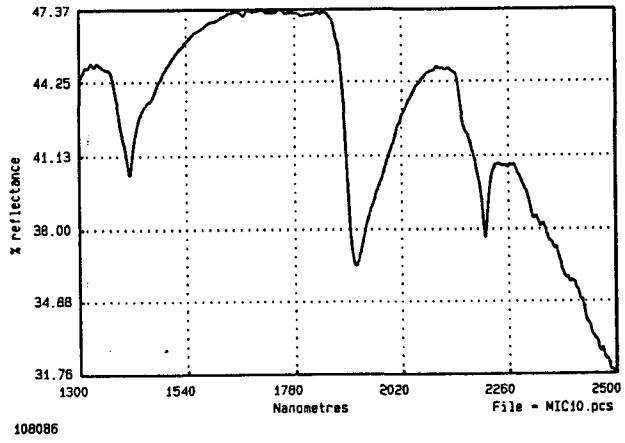

**108088**

2650 mE 4200 mN

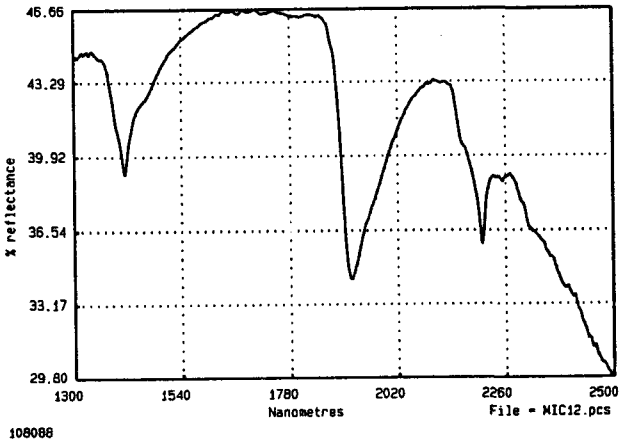


2.35 μm Absorption
nil

Oxide Abundance

| | |
|---|---|
| $SiO_2$ | 59.7% |
| $Al_2O_3$ | 11.9% |
| $Fe_2O_3$ | 6.8% |
| MgO | 2.54% |
| CaO | 3.9% |
| $Na_2O$ | 0.25% |
| $K_2O$ | 0.97% |

Mineral Abundance

| | |
|---|---|
| quartz | 6 |
| calcite | 6 |
| kaolinite | 4 |
| muscovite | 3 |
| talc | 3 |
| plagioclase | 2 |

**108089**

2643 mE 4200 mN

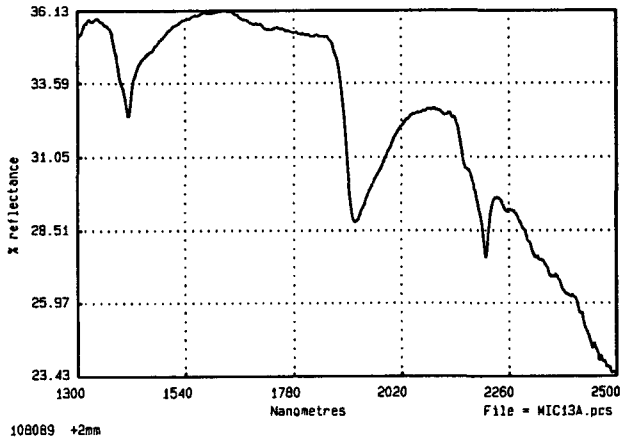


2.35 μm Absorption
nil

Oxide Abundance

| | |
|---|---|
| $SiO_2$ | 63.6% |
| $Al_2O_3$ | 9.8% |
| $Fe_2O_3$ | 6.9% |
| MgO | 2.19% |
| CaO | 4.27% |
| $Na_2O$ | 0.29% |
| $K_2O$ | 0.77% |

Mineral Abundance

| | |
|---|---|
| quartz | 6 |
| calcite | 6 |
| kaolinite | 4 |
| talc | 3 |
| plagioclase | 2 |
| musc./para. | 2 |
| verm./chlor. | 2 |
| smectite | 2 |
| paragonite | |

**108091**

2630 mE 4200 mN

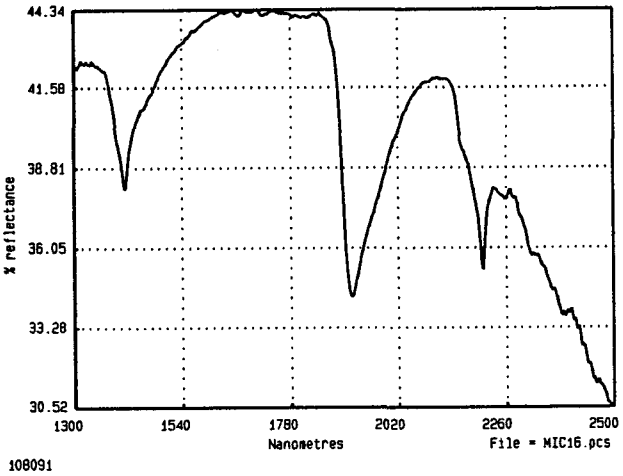


2.35 μm Absorption
nil

Oxide Abundance

| | |
|---|---|
| $SiO_2$ | 65.7% |
| $Al_2O_3$ | 10.0% |
| $Fe_2O_3$ | 9.3% |
| MgO | 1.81% |
| CaO | 1.72% |
| $Na_2O$ | 0.28% |
| $K_2O$ | 0.82% |

Mineral Abundances

| | |
|---|---|
| quartz | 6 |
| plagioclase | 6 |
| calcite | 5 |
| kaolinite | 5 |
| muscovite | 3 |
| talc | 3 |
| verm./chlor. | 1 |

**108093**

2616 mE 4200 mN

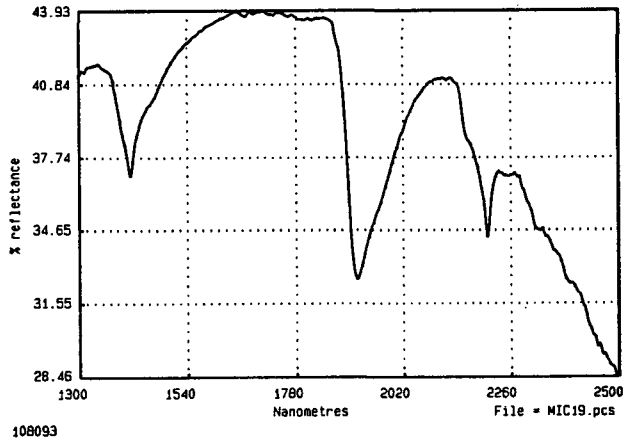


2.35 μm Absorption
nil

Oxide Abundance

| | |
|---|---|
| $SiO_2$ | 63.5% |
| $Al_2O_3$ | 10.3% |
| $Fe_2O_3$ | 7.6% |
| MgO | 2.24% |
| CaO | 3.12% |
| $Na_2O$ | 0.53% |
| $K_2O$ | 0.94% |

Mineral Abundance

| | |
|---|---|
| quartz | 6 |
| calcite | 5 |
| kaolinite | 4 |
| muscovite | 3 |
| smectite | 3 |
| plagioclase | 2 |
| talc | 2 |

**108095**

2600 mN 4200 mN

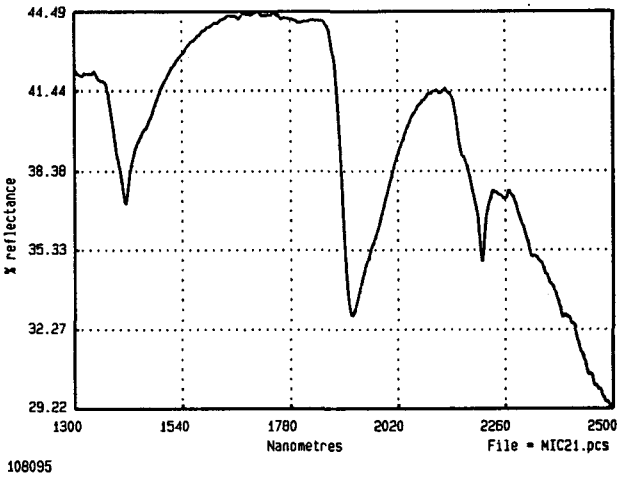


2.35 μm Absorption
nil

Oxide Abundance

| | |
|---|---|
| $SiO_2$ | 67.4% |
| $Al_2O_3$ | 9.3% |
| $Fe_2O_3$ | 7.8% |
| MgO | 2.05% |
| CaO | 2.98% |
| $Na_2O$ | 0.5% |
| $K_2O$ | 0.83% |

Mineral Abundance

| | |
|---|---|
| quartz | 6 |
| amphibole? | 6 |
| calcite | 5 |
| plagioclase | 5 |
| kaolinite | 4 |
| muscovite | 3 |
| talc | 3 |
| vermi/chlorite | 1 |
| smectite | 1 |

**108097**

2587 mE 4200 mN

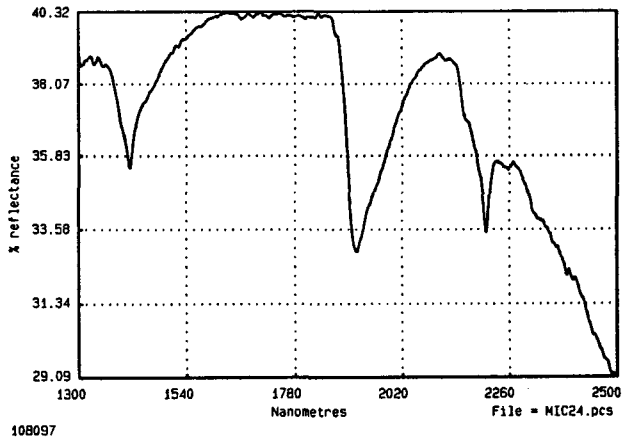


S2.35 μm Absorption
nil

Oxide Abundance

| | |
|---|---|
| $SiO_2$ | 75.1% |
| $Al_2O_3$ | 5.9% |
| $Fe_2O_3$ | 11.3% |
| MgO | 0.93% |
| CaO | 1.21% |
| $Na_2O$ | 0.35% |
| $K_2O$ | 0.53% |

Mineral Abundance

| | |
|---|---|
| quartz | 6 |
| calcite | 4 |
| kaolinite | 3 |
| plagioclase | 3 |
| muscovite | 2 |
| talc | 2 |
| smectite | 1 |

**108099**

2571 mE 4200 mN

<u>2.35 μm Absorption</u>
nil

<u>Oxide Abundance</u>

| | |
|---|---|
| $SiO_2$ | 65.7% |
| $Al_2O_3$ | 7.8% |
| $Fe_2O_3$ | 9.9% |
| MgO | 1.67% |
| CaO | 3.42% |
| $Na_2O$ | 0.39% |
| $K_2O$ | 0.63% |

<u>Mineral Abundance</u>

| | |
|---|---|
| quartz | 5 |
| calcite | 6 |
| kaolinite | 4 |
| talc | 3 |
| muscovite | 3 |
| verm./chlor. | 2 |

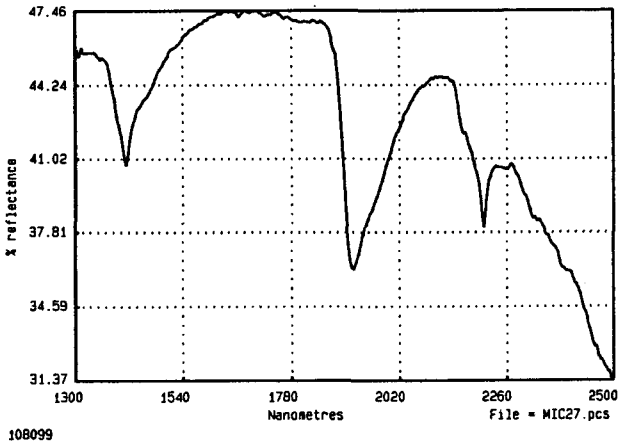


**108100**

2560 mE 4200 mN

<u>2.35 μm Absorption</u>
nil

<u>Oxide Abundance</u>

| | |
|---|---|
| $SiO_2$ | 64.5% |
| $Al_2O_3$ | 7.0% |
| $Fe_2O_3$ | 15.3% |
| MgO | 1.34% |
| CaO | 3.40% |
| $Na_2O$ | 0.17% |
| $K_2O$ | 0.50% |

<u>Mineral Abundance</u>

| | |
|---|---|
| quartz | 6 |
| calcite | 6 |
| kaolinite | 4 |
| plagioclase | 3 |
| muscovite | 2 |
| verm./chlor. | 2 |
| talc | 2 |

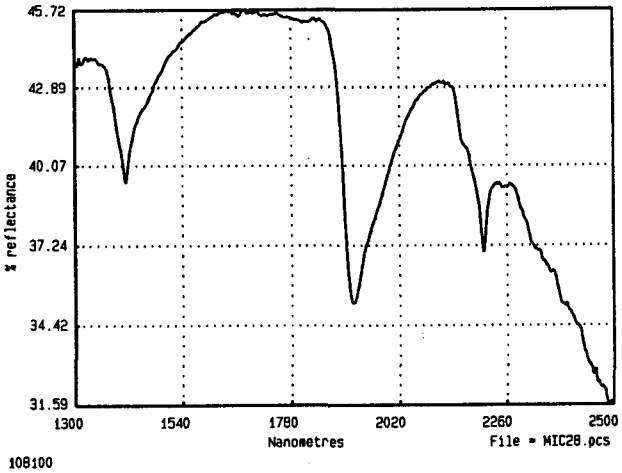

**108106**

2520 mE 4200 mN

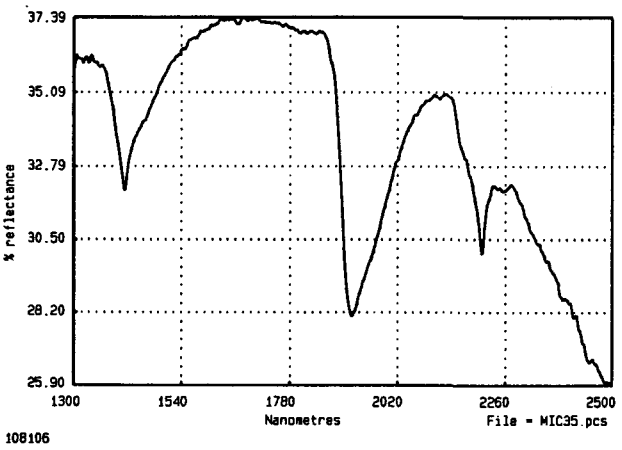


2.35 μm Absorption
nil

Oxide Abundance

| | |
|---|---|
| $SiO_2$ | 63.8% |
| $Al_2O_3$ | 9.8% |
| $Fe_2O_3$ | 15.7% |
| MgO | 1.07% |
| CaO | 0.15% |
| $Na_2O$ | 0.62% |
| $K_2O$ | 0.88% |

Mineral Abundance

| | |
|---|---|
| quartz | 6 |
| kaolinite | 4 |
| musc./para. | 2 |
| talc | 2 |
| amphibole | 1 |

**108108**

2482 mE 4200 mN

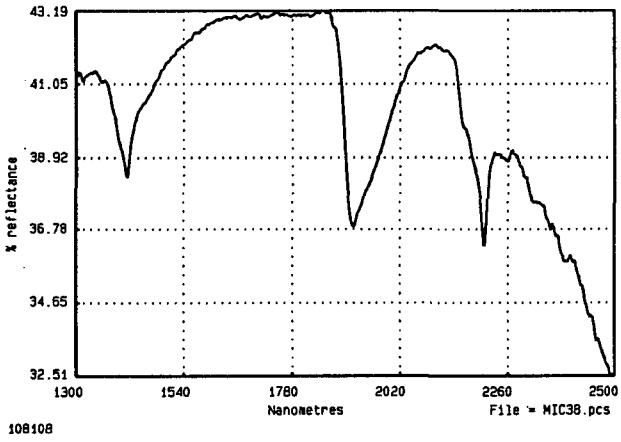


2.35 μm Absorption
nil

Oxide Abundance

| | |
|---|---|
| $SiO_2$ | 66.8% |
| $Al_2O_3$ | 9.1% |
| $Fe_2O_3$ | 16.0% |
| MgO | 0.62% |
| CaO | 0.10% |
| $Na_2O$ | 0.58% |
| $K_2O$ | 0.66% |

Mineral Abundance

| | |
|---|---|
| quartz | 6 |
| kaolinite | 5 |
| talc | 2 |
| muscovite | 1 |

**108109**

2460 mE 4200 mN

2.35 $\mu$m Absorption
nil

Oxide Abundance

| | |
|---|---|
| $SiO_2$ | 56.1% |
| $Al_2O_3$ | 8.4% |
| $Fe_2O_3$ | 11.7% |
| MgO | 3.66% |
| CaO | 3.33% |
| $Na_2O$ | 2.25% |
| $K_2O$ | 0.47% |

Mineral Abundance

| | |
|---|---|
| quartz | 6 |
| plagioclase | 6 |
| calcite | 6 |
| kaolinite | 4 |
| verm./chlor. | 3 |
| talc | 2 |
| muscovite | 1 |

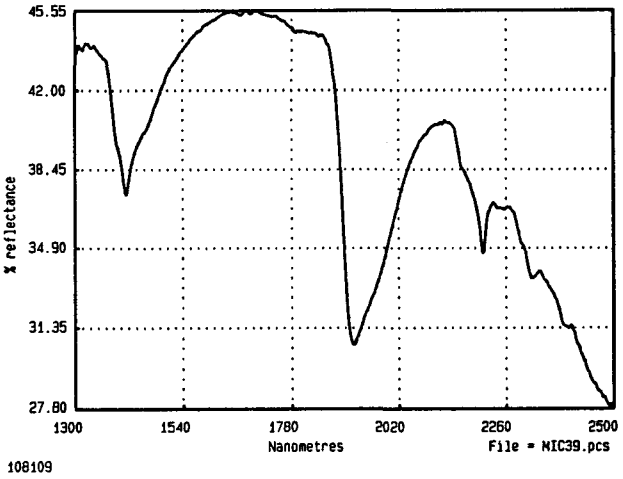


**108111**

2440 mE 4200 mN

2.35 $\mu$m Absorption
nil

Oxide Abundance

| | |
|---|---|
| $SiO_2$ | 61.7% |
| $Al_2O_3$ | 10.4% |
| $Fe_2O_3$ | 15.0% |
| MgO | 1.58% |
| CaO | 0.17% |
| $Na_2O$ | 0.82% |
| $K_2O$ | 0.71% |

Mineral Abundance

| | |
|---|---|
| quartz | 6 |
| amphibole | 6 |
| kaolinite | 5 |
| talc | 4 |
| plagioclase | 3 |
| muscovite | 3 |
| vermi/chlorite | 2 |
| smectite | 2 |

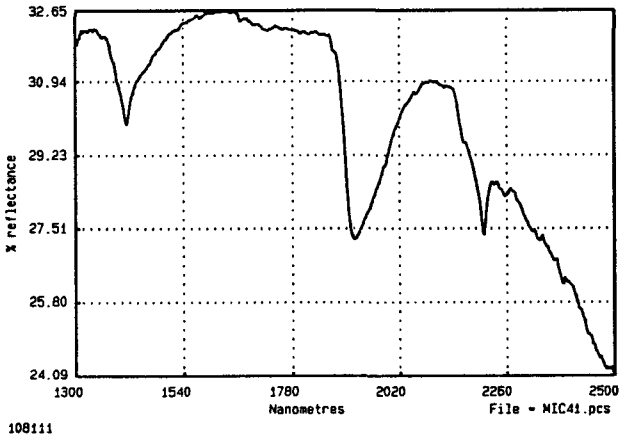

**108112**

2420 mE 4200 mN

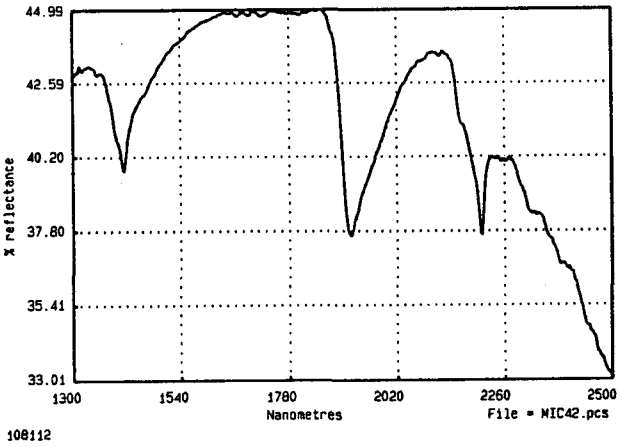


2.35 μm Absorption
nil

Oxide Abundance

| | |
|---|---|
| $SiO_2$ | 68.6% |
| $Al_2O_3$ | 7.4% |
| $Fe_2O_3$ | 16.7% |
| MgO | 1.03% |
| CaO | 0.20% |
| $Na_2O$ | 0.27% |
| $K_2O$ | 0.50% |

Mineral Abundance

| | |
|---|---|
| quartz | 6 |
| talc | 5 |
| kaolinite | 4 |
| plagioclase | 3 |
| muscovite | 2 |
| vermi/chlorite | 2 |
| smectite | 1 |

**108113**

2400 mE 4200 mN

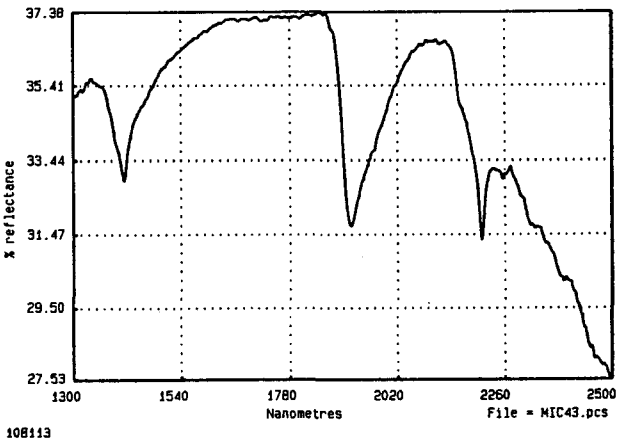


2.35 μm Absorption
nil

Oxide Abundance

| | |
|---|---|
| $SiO_2$ | 68.2% |
| $Al_2O_3$ | 8.0% |
| $Fe_2O_3$ | 15.8% |
| MgO | 1.10% |
| CaO | 0.18% |
| $Na_2O$ | 0.37% |
| $K_2O$ | 0.57% |

Mineral Abundance

| | |
|---|---|
| quartz | 6 |
| kaolinite | 5 |
| talc | 5 |
| plagioclase | 4 |
| muscovite | 3 |
| calcite | 1 |
| smectite | 1 |

**108115**
2420 mE 4300 mN
2.35 μm Absorption
nil

| Mineral Abundance | |
|---|---|
| quartz | 6 |
| kaolinite | 5 |
| talc | 5 |
| hornblende | 5 |
| plagioclase | 4 |
| muscovite | 2 |
| smectite | 2 |

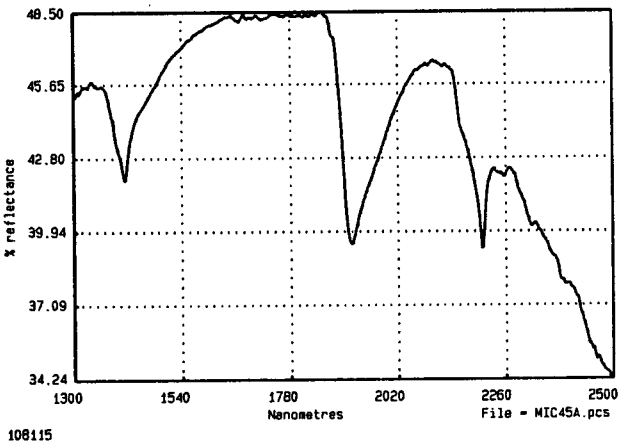

**108117**

2300 mE 4300 mN

2.35 μm Absorption
nil

Mineral Abundance

| | |
|---|---|
| quartz | 6 |
| kaolinite | 4 |
| talc | 3 |
| plagioclase | 2 |
| muscovite | 2 |
| amphibole | 2 |

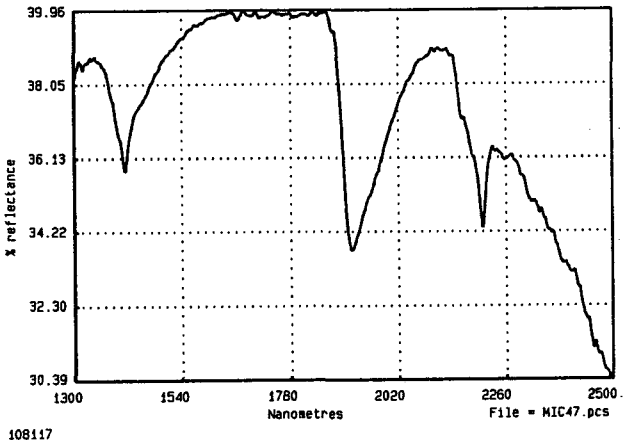


**108118**

3450 mE 4400 mN

2.35 μm Absorption
nil

Mineral Abundance

| | |
|---|---|
| gypsum | 6 |

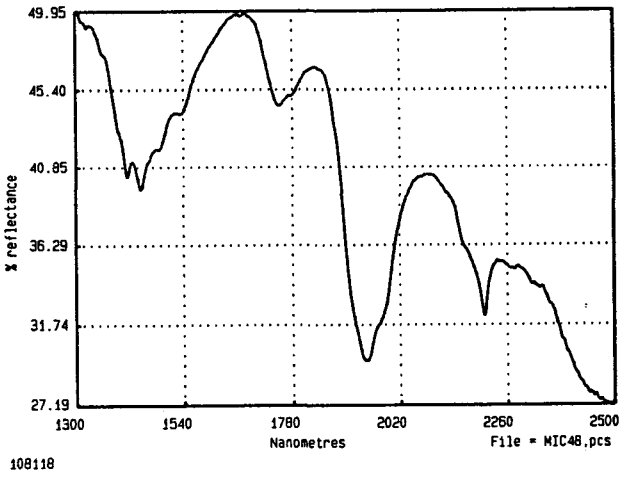

**108119**

2430 mE 5000 mN

2.35 $\mu$m Absorption
nil

Mineral Abundance

| | |
|---|---|
| quartz | 6 |
| muscovite | 2 |
| calcite | 1 |

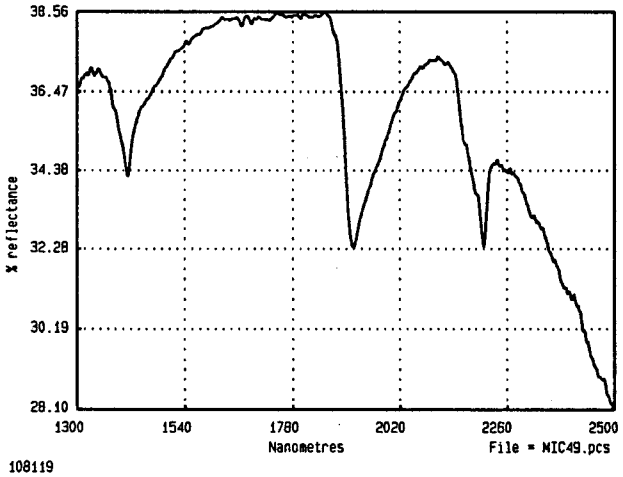

# Appendix 2

## Absorptions apparent in the PIMA-II Reflectance Spectra

The absorptions apparent in the PIMA-II spectra (Appendix 1) are listed in Table 2.1.

**Table 2.1:** ***Absorptions apparent in the spectra.***

| | Absorption ($\mu$m) |
|---|---|
| 1. | 1.360 |
| 2. | 1.398 |
| 3. | 1.411-1.430 |
| 4. | 1.450 |
| 5. | 1.472 |
| 6. | 1.764 |
| 7. | 1.871 |
| 8. | 1.918-1.940 |
| 9. | 2.120 |
| 10. | 2.165 |
| 11. | 2.196 |
| 12. | 2.202-2.212 |
| 13. | 2.255 |
| 14. | 2.318 |
| 15. | 2.351 |
| 16. | 2.384 |

The cause of these absorptions are interpreted as follows:

**1.360 $\mu$m** This minor absorption is probably related to kaolinite.

**1.398 $\mu$m** This absorption is related to kaolinite forming the characteristic absorption doublet with the 1.411.

**1.41 $\mu$m** This is a major absorption in all samples related to the OH-vibration overtone of water or dioctahedral or trioctaherdal silicates.

**1.450 $\mu$m** This absorption may be related to strongly hydrogen bonded water molecules adsorbed into the crystal lattice of minerals.

**1.764 $\mu$m** This absorption is possibly related to a sulphate mineral.

**1.870 $\mu$m** This minor absorption may be related to adsorbed water.

**1.9 μm** This absorption is related to water the wavelength of which depends on the energy environment of the OH bonds.

**2.120 μm** This weak absorption is related to dioctahedral silicates including muscovite.

**2.165 μm** This common absorption is related to kaolinite and is paired with the 2.202 μm absorption forming the characteristic kaolinite doublet at these wavelengths.

**2.174 μm** This very weak absorption is possibly related to kaolinite.

**2.194 μm** This very weak absorption is possibly related to kaolinite.

**2.202 μm** This absorption is a combination tone characteristic of dioctahedral silicates. The wavelength varies in response to the composition of the lattice and the degree of disorder.

**2.250 μm** This is a minor absorption is possibly related to Fe or Si occupying octahedral sites in the dioctahdral structure.

**2.318 μm** This absorption is related to kaolinite in these samples though the wavelength is more typical of trioctahedral silicates.

**2.350 μm** This absorption is related to the mica minerals..

**2.384 μm** This absorption is related to kaolinite in these samples though the wavelength is more typical of trioctahedral silicates.

# Appendix 3

**Interlayer and octahedral site occupation of micas from drill core samples (determined from electron microprobe analysis).**

Interlayer and octahedral site occupation of micas from drill core samples (determined from electron microprobe analysis).

| | 29635 | 39131 | 39131 | 39153 | 39153 | 39223 | 39235 | 50420 | 50420 | 50428 |
|---|---|---|---|---|---|---|---|---|---|---|
| I/layer | | | | | | | | | | |
| K | 1.50 | 0.16 | 0.17 | 0.31 | 1.45 | 1.51 | 1.54 | 1.62 | 1.19 | 1.28 |
| Na | 0.13 | 1.44 | 0.92 | 1.44 | 0.23 | 0.17 | 0.10 | 0.13 | 0.11 | 0.35 |
| Ba | 0.10 | 0.00 | 0.00 | 0.01 | 0.04 | 0.01 | 0.01 | 0.00 | 0.00 | 0.01 |
| Ca | 0.00 | 0.02 | 0.02 | 0.02 | 0.00 | 0.00 | 0.00 | 0.00 | 0.00. | 0.00 |
| Σ | 1.64 | 1.62 | 1.11 | 1.78 | 1.72 | 1.68 | 1.65 | 1.75 | 1.30 | 1.64 |
| O/hedral | | | | | | | | | | |
| Al | 3.75 | 4.01 | 4.05 | 3.88 | 3.67 | 3.88 | 3.65 | 3.79 | 3.95 | 3.70 |
| $Fe^{2+}$ | 0.20 | 0.10 | 0.27 | 0.16 | 0.17 | 0.15 | 0.20 | 0.05 | 0.05 | 0.06 |
| Mg | 0.15 | 0.01 | 0.01 | 0.01 | 0.18 | 0.07 | 0.18 | 0.21 | 0.19 | 0.15 |
| Ti | 0.03 | 0.01 | 0.00 | 0.01 | 0.01 | 0.00 | 0.02 | 0.01 | 0.02 | 0.02 |
| Σ | 4.13 | 4.13 | 4.33 | 4.06 | 4.03 | 4.10 | 4.06 | 4.08 | 4.21 | 3.93 |
| | musc. | para. | bram. | para. | musc. | musc. | musc. | musc. | illi. | Na-mus. |

musc. : muscovite
para. : paragonite
bram. : brammallite
illi. : illite
Na-mus. : Na-muscovite